



Characterization of *Sonic Hedgehog* transcripts in the adult mouse brain: co-expression with neuronal and oligodendroglial markers

Mariagiovanna Russo¹ · Giuliana Pellegrino¹ · H el ene Faure¹ · Linda Tirou¹ · Ariane Sharif² · Martial Ruat¹

Received: 31 August 2023 / Accepted: 29 December 2023 / Published online: 8 February 2024
  The Author(s) 2024

Abstract

In the adult mammalian brain, astrocytes are proposed to be the major Sonic Hedgehog (Shh)-responsive cells. However, the sources of the Shh molecule mediating activation of the pathway are still poorly characterized. The present work investigates the distribution and phenotype of cells expressing Shh mRNA in the adult mouse brain. Using single-molecule fluorescent in situ hybridization (smFISH), we report much broader expression of Shh transcripts in almost all brain regions than originally reported. We identify Shh mRNA in HuC/D⁺ neuronal populations, including GABAergic (glutamic acid decarboxylase 67, Gad67), cholinergic (choline acetyltransferase, ChAT), dopaminergic (tyrosine hydroxylase, TH), nitroergic (neuronal nitric oxide synthase, nNOS), and in a small population of oligodendroglial cells expressing Sox10 and Olig2 mRNA transcription factors. Further analysis of Shh mRNA in cerebral cortical and hypothalamic neurons suggests that Shh is also expressed by glutamatergic neurons. Interestingly, we did not observe substantial Desert Hedgehog and Indian Hedgehog mRNA signals, nor Shh signals in S100 ⁺ astrocytes and Iba1⁺ microglial cells. Collectively, the present work provides the most robust central map of Shh-expressing cells to date and underscores the importance of nitroergic neurons in regulating Shh availability to brain cells. Thus, our study provides a framework for future experiments aimed at better understanding of the functions of Shh signaling in the brain in normal and pathological states, and the characterization of novel regulatory mechanisms of the signaling pathway.

Keywords RNAscope · Neurodegenerative diseases · Multiple sclerosis · Patched · Shh · Smoothed

Introduction

The early discovery of Sonic Hedgehog (Shh) transcript expression in mature rodent brain neurons (Traiffort et al. 1998, 1999) paved the way for further studies on the role of Shh signaling in the mammalian brain under physiological conditions or during disease (Briscoe and Therond 2013; Ferent et al. 2013b; Alvarez-Buylla and Ihrie 2014; Ruat et al. 2015; Yao et al. 2016; Garcia et al. 2018; Laouarem and Traiffort 2018; Garcia 2021; Laouarem et al. 2021). Studies in rodents have highlighted a primary role for the pathway in regulating neurogenic niches in the subventricular zone of the lateral ventricles (SVZ) and the subgranular zone (SGZ) of the hippocampus, and the status of oligodendroglial progenitors in brain and cortical structures. Positive modulation of the Shh signaling pathway has been proposed as a potential therapeutic approach for Parkinson's disease (Gonzalez-Reyes et al. 2012; Malave et al. 2021) and for demyelinating diseases (Loulier et al. 2006; Ferent et al. 2013b; Porcu et al. 2015; Samanta et al. 2015; Del Giovane

  Martial Ruat
martial.ruat@cnr.fr

Mariagiovanna Russo
mariagiovanna.russo@universite-paris-saclay.fr

Giuliana Pellegrino
g8.pellegrino@gmail.com

H el ene Faure
helene.faure@cnr.fr

Linda Tirou
tirou.linda@yahoo.com

Ariane Sharif
ariane.sharif@inserm.fr

¹ CNRS, Paris-Saclay University, UMR-9197, Neuroscience Paris-Saclay Institute, 91400 Saclay, France

² Univ. Lille, Inserm, CHU Lille, Laboratory of Development and Plasticity of the Neuroendocrine Brain, Lille Neuroscience and Cognition, UMR-S 1172, FHU 1000 Days for Health, Lille, France

et al. 2022). Blocking the pathway by small molecules inhibitors of the GTP-binding protein-coupled receptor Smoothed (Smo) is proposed as an alternative for treating Shh-dependent medulloblastoma, a cerebellar tumor with a poor prognosis in children (Ruat et al. 2014; Swiderska-Syn et al. 2022). Genetic mutations affecting genes associated with Shh signaling are responsible for the developmental diseases such as holoprosencephaly or medulloblastoma (Wolter et al. 1997; Reifenberger et al. 1998; Traiffort et al. 2004; Ruat et al. 2015; Andreu-Cervera et al. 2021).

Shh belongs to a family of secreted morphogens including Desert Hedgehog (Dhh) and Indian Hedgehog (Ihh). These molecules are synthesized as precursors that undergo internal cleavage generating an aminoterminal peptide displaying almost all biological activities of the peptides. Binding of Shh to its receptor Patched (Ptc), a member of the Resistance-Nodulation-Division transporter superfamily, activates Smo (Ruat et al. 2014; Zhang and Beachy 2023). These events result in complex modulation of the zinc-finger transcription factors glioma-associated oncogenes 1–3 (Gli1–3). Shh is widely distributed in rodent brain regions, whereas Dhh and Ihh expression has not been detected (Ruat et al. 2015; Garcia et al. 2018). Astrocytes have been proposed as the primary targets of Shh signaling as they express components of the Shh transduction machinery including Ptc, Smo, and Gli1–3 (Garcia et al. 2010, 2018; Ruat et al. 2015; Allahyari et al. 2019; Hill et al. 2019; Tirou et al. 2021; Wang et al. 2021). However, the discrepancy between the expression of Ptc and Smo transcripts in several brain areas has led to the hypothesis that Ptc may transduce the Shh signal in the absence of Smo and that Smo may be activated by non-canonical mechanisms (Traiffort et al. 1998; Charytoniuk et al. 2002). It has been reported by us and other groups that both Ptc and Smo are expressed in neurons (Alvarez-Buylla and Ihrie 2014; Ruat et al. 2015; Garcia et al. 2018). The initial discovery of cells expressing Shh transcripts using specific digoxigenin-labeled riboprobes in rodent brain (Traiffort et al. 1998) was followed by detailed analysis of cells expressing this marker in mature rodent central nervous system under physiological and pathophysiological conditions. These studies were conducted with Shh-reporter mouse lines, Shh antibodies, or radioactive and cold riboprobes (Traiffort et al. 1998; Traiffort et al. 2001; Charytoniuk et al. 2002; Lai et al. 2003; Machold et al. 2003; Desouza et al. 2011; Ihrie et al. 2011; Eitan et al. 2016; Sanchez and Armstrong 2018; Sanchez et al. 2018; Gonzalez-Reyes et al. 2019; Rivell et al. 2019; Tirou et al. 2020; Tu et al. 2023). Thus, it has been proposed that Shh is synthesized by a subpopulation of GABAergic cells expressing Gad67 in the ventral brain, by a restricted population of cholinergic neurons expressing ChAT in the motor nuclei and in the basal forebrain (Traiffort et al.

1999; Pascual et al. 2005; Ihrie et al. 2011), by cerebral cortical neurons mainly located in layer V of the cerebral cortex (Charytoniuk et al. 2002; Harwell et al. 2012), in dopaminergic neurons of the substantia nigra (Gonzalez-Reyes et al. 2012; Turcato et al. 2022), in a population of hilar cells (McMahon et al. 2003; Gonzalez-Reyes et al. 2019), in some Pomc⁺ cells of the arcuate nucleus (ARC) and some Mchr1⁺ cells of the paraventricular nucleus (PVN) in the hypothalamus (Antonellis et al. 2021), and in Purkinje cells of the cerebellum (Traiffort et al. 1998; Wallace 1999; Farmer et al. 2016). Several ventral brain regions, including the hypothalamic and thalamic nuclei, have also been reported to express Shh signaling (Garcia et al. 2010; Antonellis et al. 2021; Tirou et al. 2021). In most of these studies, Shh is expressed by neurons, while Shh expression in astrocytes and microglia has been observed occasionally in physiological conditions (Sanchez and Armstrong 2018); whereas, Shh expression in these cells under pathophysiological conditions required further investigations (Ruat et al. 2015; Yao et al. 2016; Garcia et al. 2018; Laouarem and Traiffort 2018; Garcia 2021).

Recently, we reported broad expression of Shh recognized by the specific monoclonal antibody C9C5 in a subset of mature CC1⁺ oligodendrocytes (Tirou et al. 2020). We also identified Shh transcripts by single-molecule fluorescent in situ hybridization (smFISH) in a subset of cells expressing the oligodendroglial markers Olig2 and Sox10 mRNA. These results revealed that Shh expression was more extensive than originally reported. Now, we report a much broader expression of Shh transcripts in the mature mouse brain, which occurs in diverse neuronal populations and in a restricted population of oligodendroglial cells. We also identified a new population of neurons co-expressing Shh transcripts and the nitrergic marker nNOS and reported broad expression of Shh transcripts in hypothalamic nuclei, suggesting potential new roles for Shh in the regulation of neural circuits.

Materials and methods

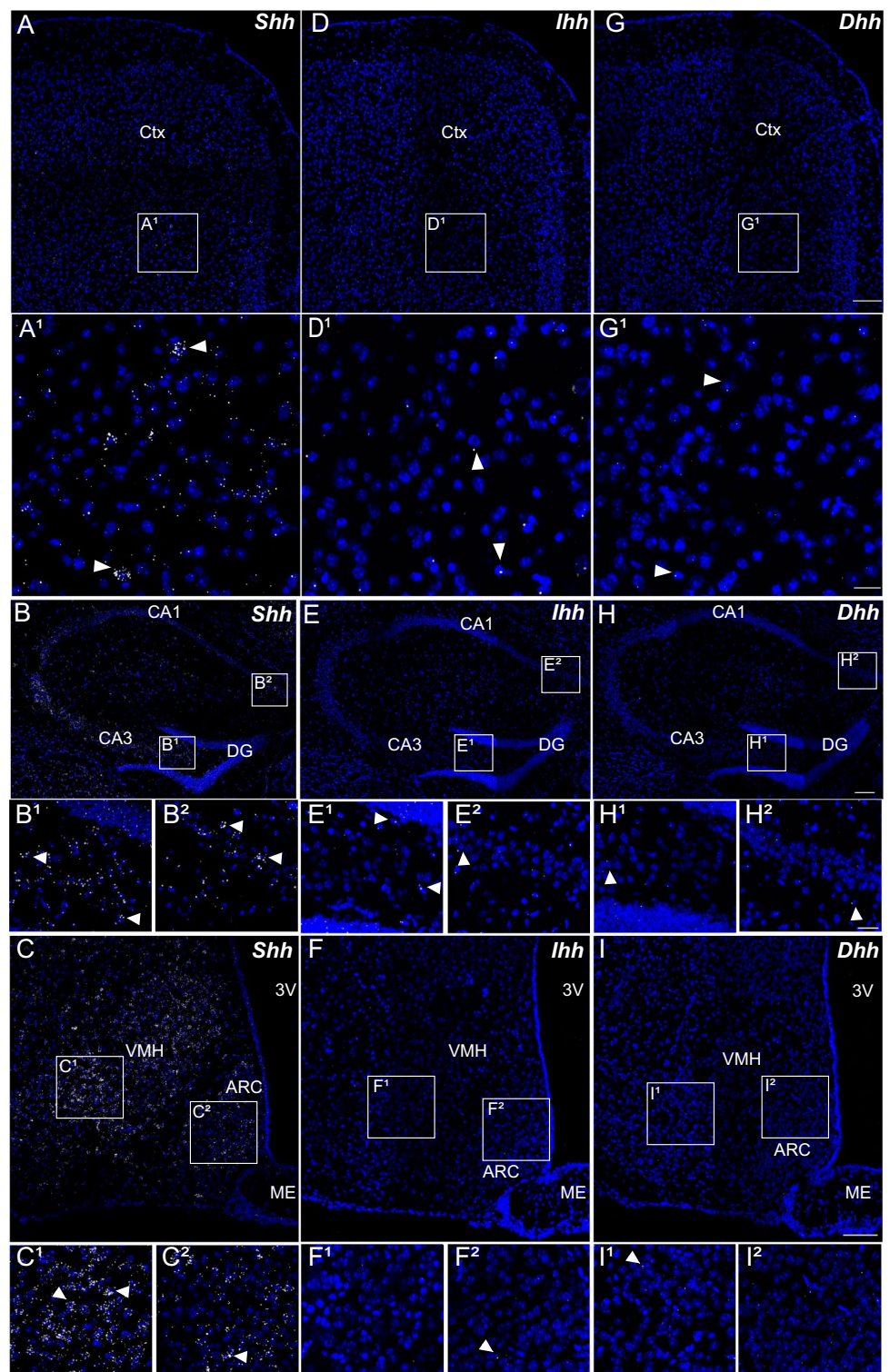
Ethical approval

All animal experiments were performed in accordance with the Council Directive 2010/63EU of the European Parliament and were approved (Project No. 4558) by the French ethic committee.

Mice and tissue preparation

Young adult (2–3 months old) rodent have been used previously for reporting expression of Shh or its signaling

Fig. 1 Representative images of *Shh*, *Dhh*, and *Ihh* transcripts distribution by in situ hybridization in distinct adult mouse brain regions. *Shh* transcripts are identified in the cerebral cortex (Ctx) (A), in various layers of the hippocampus (B) and in hypothalamic nuclei (C). The highest expression is observed in cells located in layer V of the cerebral cortex (A1), in CA3 (B1) and CA1 (B2) layers of the hippocampus, in the ventromedial hypothalamic nucleus (VMH) (C1) and the arcuate hypothalamic nucleus (ARC) (C2). Rare *Ihh* and *Dhh* transcripts are present in the cerebral cortex (D, G), in the hippocampus region (E, H), and in hypothalamic nuclei (F, I). A1–I2 are high magnification views of indicated boxed areas in the main panels. Arrowheads show cells associated to one (*Ihh*, *Dhh*) or more (*Shh*) dots. Sections are counterstained using DAPI to visualize cell nuclei. *LV* lateral ventricle, *DG* dentate gyrus of the hippocampus, *ME* median eminence, *3V* third ventricle. Scale bars: A–I = 100 μ m; A1–I2 = 20 μ m



components (Ruat et al. 2015; Laouarem et al. 2018; Garcia 2021). Thus, young adult (2–3 months old) C57Bl/6J (Janvier-Labs) were housed grouped and maintained with access to food and water ad libitum. The room had constant temperature (21–22 °C) and a 12:12-h light/dark cycle. Mice were deeply anesthetized with intraperitoneal injection of

xylazine 4 mg/kg (Sedaxylan, Chetra) and ketamine 20 mg/kg (Ketalar, Parke-Davis), and were perfused with 4% paraformaldehyde (PFA) in 0.2 M sodium phosphate, pH 7.4. After dissection, brains were post-fixed for 2 h in 4% PFA and cryoprotected in 20% sucrose/PBS waiting for the tissue to sink at the bottom of the tube. The tissues were mounted

Table 1 Distribution of *Shh* transcripts in the mouse brain

Region	Nucleus		
Cortex	Layer I	1 ⁺	
	Layer II/III	1 ⁺ –3 ⁺	
	Layer IV	1 ⁺ –2 ⁺	
	Layer V	1 ⁺ –3 ⁺	
	Layer VIa	1 ⁺ –3 ⁺	
	Layer VIb	1 ⁺ –3 ⁺	
	Clastrum	1 ⁺ –4 ⁺	
Hippocampus	CA1	1 ⁺ –3 ⁺	
	CA2	1 ⁺ –3 ⁺	
	CA3	1 ⁺ –3 ⁺	
	Dentate gyrus		
	Granul cell layer	1 ⁺ –3 ⁺	
	Polymorph layer	1 ⁺ –2 ⁺	
	Molecular layer	1 ⁺ –2 ⁺	
Striatum	Caudate putamen	1 ⁺ –4 ⁺	
	Anterior amygdala area	1 ⁺ –4 ⁺	
Pallidum	Globus pallidus	1 ⁺ –4 ⁺	
	Magnocellular preoptic nucleus	1 ⁺ –4 ⁺	
	Medial septal nucleus	1 ⁺ –3 ⁺	
	Lateral septal nucleus	1 ⁺ –4 ⁺	
Thalamus	Medial habenular nucleus	1 ⁺	
	Lateral habenular nucleus	1 ⁺ –3 ⁺	
	Paraventricular nucleus	1 ⁺ –3 ⁺	
	Mediodorsal nucleus	1 ⁺ –3 ⁺	
	Intermediodorsal nucleus	1 ⁺ –3 ⁺	
	Centrolateral nucleus	1 ⁺ –3 ⁺	
	Paracentral nucleus	1 ⁺ –2 ⁺	
	Central medial nucleus	1 ⁺ –3 ⁺	
	Lateral posterior nucleus	1 ⁺ –3 ⁺	
	Dorsolateral geniculate nucleus	1 ⁺	
	Lateral dorsal nucleus	1 ⁺	
	Posterior nucleus	1 ⁺ –3 ⁺	
	Ventral nucleus		
		Antero-lateral	1 ⁺ –2 ⁺
		Postero-lateral	1 ⁺
		Medial	1 ⁺ –3 ⁺
	Postero-medial	1 ⁺ –2 ⁺	
	Reticular nucleus	1 ⁺	
	Rhomboid nucleus	1 ⁺ –3 ⁺	
	Submedius nucleus	1 ⁺ –3 ⁺	
	Xiphoid nucleus	1 ⁺ –2 ⁺	
	Reuniens nucleus	1 ⁺ –2 ⁺	
	Ventral reuniens nucleus	1 ⁺ –2 ⁺	
Hypothalamus	Arcuate hypothalamic nucleus		
		Dorsal part	1 ⁺ –3 ⁺
		Ventral part	1 ⁺ –3 ⁺
	Ventromedial hypothalamic nucleus		
		Dorsomedial part	1 ⁺ –3 ⁺
		Central part	1 ⁺ –3 ⁺
	Ventromedial part	1 ⁺ –3 ⁺	
	Dorsomedial hypothalamic nucleus	1 ⁺ –3 ⁺	

Table 1 (continued)

Region	Nucleus	
	Posterior hypothalamic nucleus	1 ⁺ –3 ⁺
	Lateral hypothalamic nucleus	
		Anterior 1 ⁺ –3 ⁺
		Posterior 1 ⁺ –3 ⁺
	Median eminence	1 ⁺
	Tuberal nucleus	1 ⁺ –2 ⁺
	Anterior hypothalamic nucleus	1 ⁺ –2 ⁺
	Sub-paraventricular zone	1 ⁺ –3 ⁺
	Paraventricular hypothalamic nucleus	1 ⁺ –3 ⁺
	Suprachiasmatic nucleus	1 ⁺
	Optic chiasma	1 ⁺
	Mammillary body	1 ⁺ –3 ⁺
Midbrain	Ventral tegmental area	1 ⁺ –3 ⁺
	Substantia nigra, pars compacta	1 ⁺ –3 ⁺
	Substantia nigra, pars reticulata	1 ⁺ –3 ⁺
Pons	Mesencephalic trigeminal nucleus	1 ⁺ –4 ⁺
	Pontine central gray	1 ⁺ –3 ⁺
	Motor trigeminal nucleus	1 ⁺ –4 ⁺
Medulla	Facial nucleus	1 ⁺ –4 ⁺
	Intermediate reticular nucleus	1 ⁺ –3 ⁺
	Gigantocellular reticular nucleus	1 ⁺ –3 ⁺
	Parapyramidal nucleus	1 ⁺ –2 ⁺
Cerebellum	Granule cell layer	1 ⁺
	Purkinje cell layer	4 ⁺
	Molecular layer	1 ⁺
	White matter	1 ⁺

Density of *Shh* mRNA was estimated by smFISH from $N=3-4$ animals. 4+: very high density, >30 dots/cell; 3+: high density, 10–30 dots/cell; 2+: moderate density, 6–9 dots/cell; 1+: low density, 2–5 dots/cell. Nuclei associated to one dot were observed scattered in all regions. *Shh*-transcript expression was considered as “undetectable” in these cells

in Optimal Cutting Temperature (O.C.T.) compound Tissue-Tek (Sakura Finetek), frozen in liquid nitrogen-cooled isopentane and kept at -80°C until use. Tissues were allowed to equilibrate to -20°C in the cryostat (Leica, CM3050) for ~30 min and 14 μm coronal sections were mounted onto SuperFrost[®] ultra Plus slides (Thermo Scientific), dried for 1–2 h at -20°C and stored at -80°C for less than three months. Anatomical landmarks were determined using a mouse brain atlas (Paxinos and Franklin 2001).

RNAscope[®] in situ multiplex fluorescent assay

The RNAscope Multiplex Fluorescent v2 Reagent Kit was used according to the manufacturer’s instructions (Advanced Cell Diagnostics) with minor modifications. Slides were post-fixed in 4% PFA for 30 min, and then washed in sterile PBS (2 \times 5 min) followed by dehydration in increasing

concentrations of ethanol (50%, 70%, 100%) for 5 min each at room temperature. Then, slides were air-dried for 5 min and incubated for 30 min at 37°C in a humidified chamber. Sections were then pretreated with hydrogen peroxide (10 min) and antigen retrieval was performed for 15 min at 98°C . After 5-min drying at room temperature, a hydrophobic barrier was drawn around the brain sections with ImmEdge Pen and they were dried again for 5 min. Sections were treated with RNAscope[®] Protease Plus, and incubated with hybridization probes and amplifiers. Positive and negative control probes were run in each experiment as an internal control, to assess sample RNA quality and tissue optimal permeabilization. Development of HRP signal with TSA[®] plus fluorophores was performed exactly as recommended with the dilution indicated in Table S1. Finally, slides were counterstained with RNAscope[®] Multiplex FI v2 DAPI. Images were acquired with a 20 \times objective using an Axio Imager Z2 ApoTome microscope equipped with a motorized

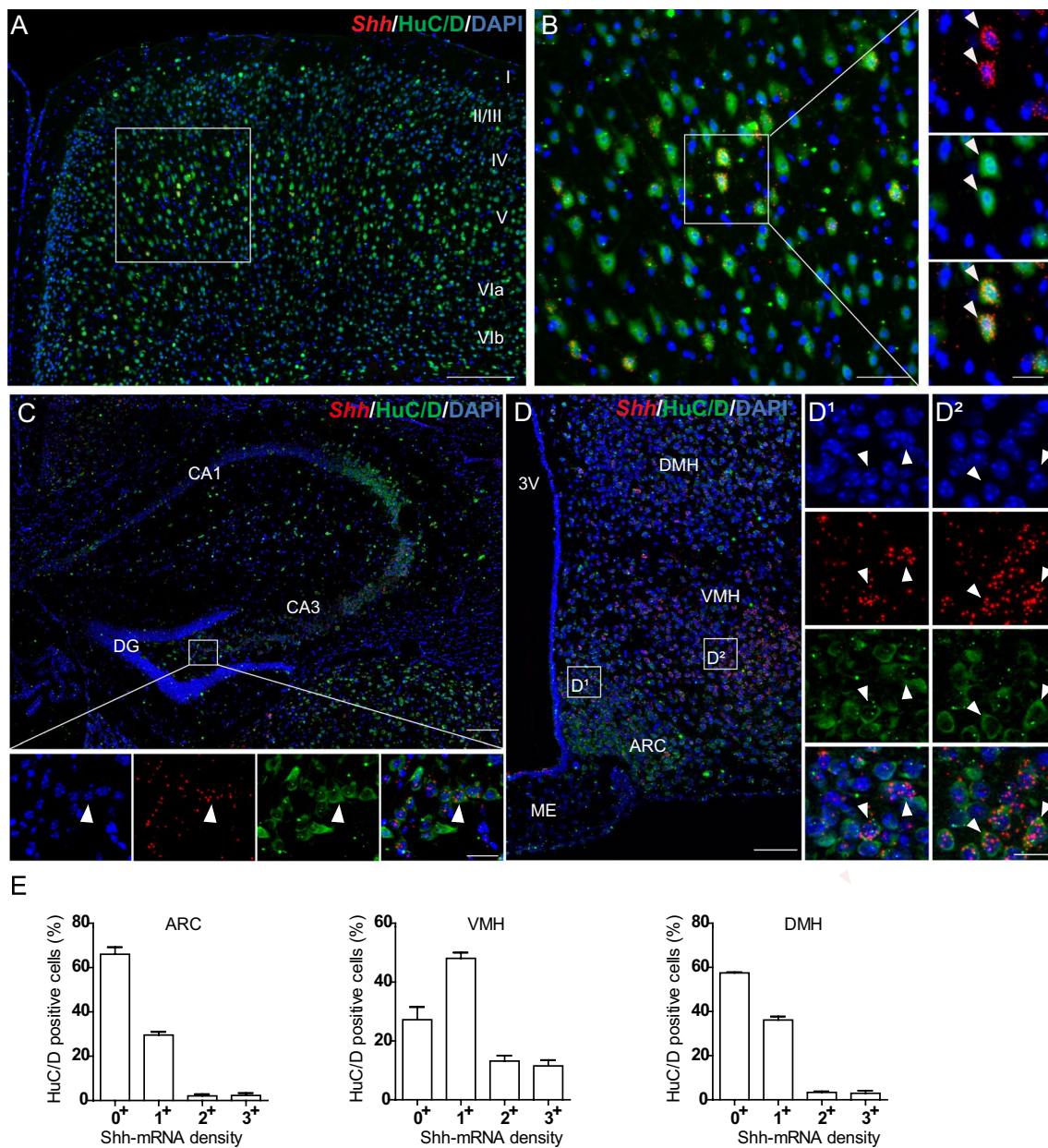


Fig. 2 Representative images of fluorescent in situ hybridization of *Shh* (red) combined with immunofluorescence for the neuronal marker HuC/D (green), in mouse cerebral cortical layers (**A**, **B**), hippocampus (**C**) and mediobasal hypothalamus (**D–D2**). *Shh* is detected with varying intensity level in neurons expressing HuC/D showing the highest expression in cortical layer V (**B**), in the arcuate hypothalamic nucleus (ARC) and ventromedial hypothalamic nucleus (VMH) (**D1–D2**). **B** is the magnification of boxed area in **A**. White square in **C** is magnified below the main panel. Arrowheads show *Shh* positive cells represented in single and merged channels with

the nuclear marker DAPI (blue). Percentage of HuC/D⁺ neurons expressing different level of *Shh* mRNA density was quantified in the ARC, the VMH and the dorsomedial hypothalamic nucleus (DMH). Mean ± SEM. Density of *Shh* mRNA was estimated by RNAscope from $N=3$ animals. More than 100 HuC/D-expressing cells were counted per animal in each of the three regions analyzed (**E**). *DG* dentate gyrus of the hippocampus, *3V* third ventricle, *ME* median eminence. Scale bars: **A** = 200 μ m; **B–D** = 100 μ m; **D1–D2** = 20 μ m; all magnifications = 20 μ m

stage (Zeiss, Germany) or a fluorescence microscope Leica DM2000. All images were captured over a defined z-focus range corresponding to visible fluorescence within the

section. Negative controls were used to assess the negative control background and to set the signal-to-noise ratio for background levels for each experiments. Positive controls

Table 2 Distribution of *Shh* transcripts in the neuronal population of the mouse brain

Region	Nucleus	HuC/D	<i>Gad67</i>	<i>ChAT</i>	<i>nNOS</i>	TH
Cortex	Layer I	1 ⁺	1 ⁺	0 ⁺	1 ⁺	n.d.
	Layer II/III	1 ⁺ –3 ⁺	1 ⁺ –3 ⁺	0 ⁺	1 ⁺ –2 ⁺	n.d.
	Layer IV	1 ⁺ –2 ⁺	1 ⁺	0 ⁺	1 ⁺	n.d.
	Layer V	1 ⁺ –3 ⁺	1 ⁺ –3 ⁺	0 ⁺	1 ⁺ –3 ⁺	n.d.
	Layer VIa	1 ⁺ –3 ⁺	1 ⁺ –2 ⁺	0 ⁺	1 ⁺ –3 ⁺	n.d.
	Layer VIb	1 ⁺ –3 ⁺	1 ⁺ –2 ⁺	0 ⁺	1 ⁺	n.d.
Hippocampus	CA1	1 ⁺ –3 ⁺	1 ⁺ –3 ⁺	/	1 ⁺	n.d.
	CA2	1 ⁺ –3 ⁺	1 ⁺ –3 ⁺	/	1 ⁺	n.d.
	CA3	1 ⁺ –3 ⁺	1 ⁺ –3 ⁺	/	1 ⁺ –3 ⁺	n.d.
	Dentate gyrus					
	Granul cell layer	1 ⁺ –3 ⁺	/	/	1 ⁺	n.d.
	Polymorph layer	1 ⁺ –2 ⁺	1 ⁺ –2 ⁺	/	1 ⁺	n.d.
	Molecular layer	1 ⁺ –2 ⁺	1 ⁺ –2 ⁺	/	1 ⁺	n.d.
Striatum	Caudate putamen	1 ⁺ –3 ⁺	1 ⁺ –3 ⁺	0 ⁺	n.d.	n.d.
Pallidum	Globus pallidus	n.d.	1 ⁺ –4 ⁺	0 ⁺	n.d.	n.d.
	Magnocellular preoptic nucleus	n.d.	1 ⁺ –4 ⁺	1 ⁺ –3 ⁺	n.d.	n.d.
Hypothalamus	Arcuate hypothalamic nucleus					
	Dorsal part	1 ⁺ –3 ⁺	1 ⁺ –3 ⁺	1 ⁺	1 ⁺ –3 ⁺	n.d.
	Ventral part	1 ⁺ –3 ⁺	1 ⁺ –3 ⁺	1 ⁺	1 ⁺ –2 ⁺	n.d.
	Ventromedial hypothalamic nucleus					
	Dorsomedial part	1 ⁺ –3 ⁺	1 ⁺ –3 ⁺	1 ⁺	1 ⁺ –3 ⁺	n.d.
	Central part	1 ⁺ –3 ⁺	1 ⁺	1 ⁺	1 ⁺ –3 ⁺	n.d.
	Ventromedial part	1 ⁺ –3 ⁺	1 ⁺	/	1 ⁺ –3 ⁺	n.d.
	Dorsomedial hypothalamic nucleus	1 ⁺ –3 ⁺	1 ⁺ –3 ⁺	1 ⁺	1 ⁺ –3 ⁺	n.d.
	Posterior hypothalamic nucleus	1 ⁺ –3 ⁺	1 ⁺ –3 ⁺	1 ⁺	1 ⁺	n.d.
	Lateral hypothalamic nucleus					
	Anterior	n.d.	1 ⁺ –3 ⁺	/	n.d.	n.d.
	Posterior	1 ⁺ –3 ⁺	1 ⁺ –3 ⁺	0 ⁺	1 ⁺ –3 ⁺	n.d.
	Posterior	1 ⁺ –3 ⁺	1 ⁺ –3 ⁺	0 ⁺	1 ⁺ –3 ⁺	n.d.
	Median eminence	1 ⁺ –2 ⁺	0 ⁺	/	0 ⁺	n.d.
	Tuberal nucleus	1 ⁺ –2 ⁺	1 ⁺ –2 ⁺	0 ⁺	1 ⁺	n.d.
	Anterior hypothalamic nucleus	n.d.	1 ⁺ –2 ⁺	/	n.d.	n.d.
	Sub-paraventricular zone	n.d.	1 ⁺ –3 ⁺	/	n.d.	n.d.
	Paraventricular hypothalamic nucleus	n.d.	1 ⁺ –2 ⁺	/	n.d.	n.d.
	Suprachiasmatic nucleus	n.d.	1 ⁺	/	n.d.	n.d.
Optic chiasma	n.d.	/	/	n.d.	n.d.	
Midbrain	Ventral tegmental area	n.d.	n.d.	n.d.	n.d.	1 ⁺ –3 ⁺
	Substantia nigra, pars compacta	n.d.	n.d.	n.d.	n.d.	1 ⁺ –3 ⁺
	Substantia nigra, pars reticulata	n.d.	n.d.	n.d.	n.d.	/
Pons	Mesencephalic trigeminal nucleus	n.d.	1 ⁺	4 ⁺	1 ⁺ –3 ⁺	n.d.
	Pontine central gray	n.d.	1 ⁺ –3 ⁺	1 ⁺ –3 ⁺	1 ⁺ –3 ⁺	n.d.
	Motor trigeminal nucleus	n.d.	1 ⁺ –2 ⁺	4 ⁺	/	n.d.
Medulla	Facial nucleus	n.d.	1 ⁺ –2 ⁺	4 ⁺	1 ⁺ –3 ⁺	n.d.
	Intermediate reticular nucleus	n.d.	1 ⁺ –2 ⁺	/	1 ⁺ –3 ⁺	n.d.
	Gigantocellular reticular nucleus	n.d.	1 ⁺ –3 ⁺	/	1 ⁺ –3 ⁺	n.d.
	Parapyramidal nucleus	n.d.	1 ⁺	/	/	n.d.
Cerebellum	Granule cell layer	n.d.	1 ⁺	/	0 ⁺	n.d.
	Purkinje cell layer	n.d.	4 ⁺	/	/	n.d.
	Molecular layer	n.d.	1 ⁺	/	1 ⁺	n.d.
	White matter	n.d.	1 ⁺	/	/	n.d.

Density of *Shh* mRNA was estimated by smFISH from N=3–4 animals. 4⁺: highest density, > 20 dots/cell; 3⁺: high density, 10–20 dots/cell; 2⁺: moderate density, 6–9 dots/cell; 1⁺: low density, 2–5 dots/cell; 0⁺: undetectable, 0–1 dot/cell; /: not relevant; n.d.: not determined

Table 3 Percentage of *Shh* transcripts expressing cells in HuC/D⁺, GABAergic *Gad67*⁺, and nitroergic *nNOS*⁺ neuronal populations of the mouse cortex and arcuate, ventromedial and dorsomedial hypothalamic nuclei

Region	<i>Shh</i> ⁺ cells (% ± SEM) ^a		
	HuC/D	<i>Gad67</i>	<i>nNOS</i>
Cortex	29.6 ± 3.3	5.9 ± 0.6	1.8 ± 0.2
Hypothalamus			
Arcuate	34.0 ± 3.2	36.1 ± 5.8	28.1 ± 3.7
Ventromedial hypothalamic nucleus	72.8 ± 4.3	n.d.	56.4 ± 5.8
Dorsomedial hypothalamic nucleus	42.5 ± 0.3	56.2 ± 7.1	37.6 ± 1.1

The percentage is reported as mean ± SEM and was estimated by smFISH from *N* = 3 animals. More than 100 cells were counted per animal in each of the region analyzed. *n.d.* not determined

^aScattered *ChAT*⁺ cells expressing low *Shh* (1⁺) were observed in the arcuate, ventromedial hypothalamic nucleus, and the dorsomedial hypothalamic nucleus

were used to assess the positive control signal strength. Images were analyzed using ZEN software (Zeiss) or LAS-X software (Leica) and reconstructed in ImageJ 1.52p (NIH) using the z-stack module and Photoshop CS3 (Adobe).

Immunohistochemistry

Some sections were subjected to immunohistochemistry after RNAscope and before counterstaining. They were blocked 1 h in PBS, 0.25% Triton-X100, 1% BSA. After washing in PBS pH 7.4 (2 × 5 min), the primary antibodies, detailed in Supplementary Information Table S2, were incubated at 4 °C overnight for anti-S100β and anti-HuC/D or for 2 nights for anti-TH. Next, slices were washed in PBS (3 × 5 min) and incubated with the secondary antibody (1/400, 488-conjugated Donkey, anti-mouse (# R37114) or anti rabbit (#R37118), Invitrogen) for 2 h at room temperature. Finally, slides were washed again in PBS (3 × 5 min) and counterstained with RNAscope® Multiplex FI v2 DAPI to be analyzed as described above. Association of in situ probes and antibodies is listed in Supplementary Information Table S3 together with sagittal position to bregma of the sections analyzed.

Cell count and analysis

Brain regions were delineated using the Allen Adult Mouse Brain Atlas (<http://atlas.brain-map.org/atlas=602630314#atlas=602630314&>). The nomenclature used corresponds to the one described in the Paxinos Atlas. The quantification of HuC/D-, *Gad67*-, *nNOS*-, and TH-expressing neurons was done by counting the number

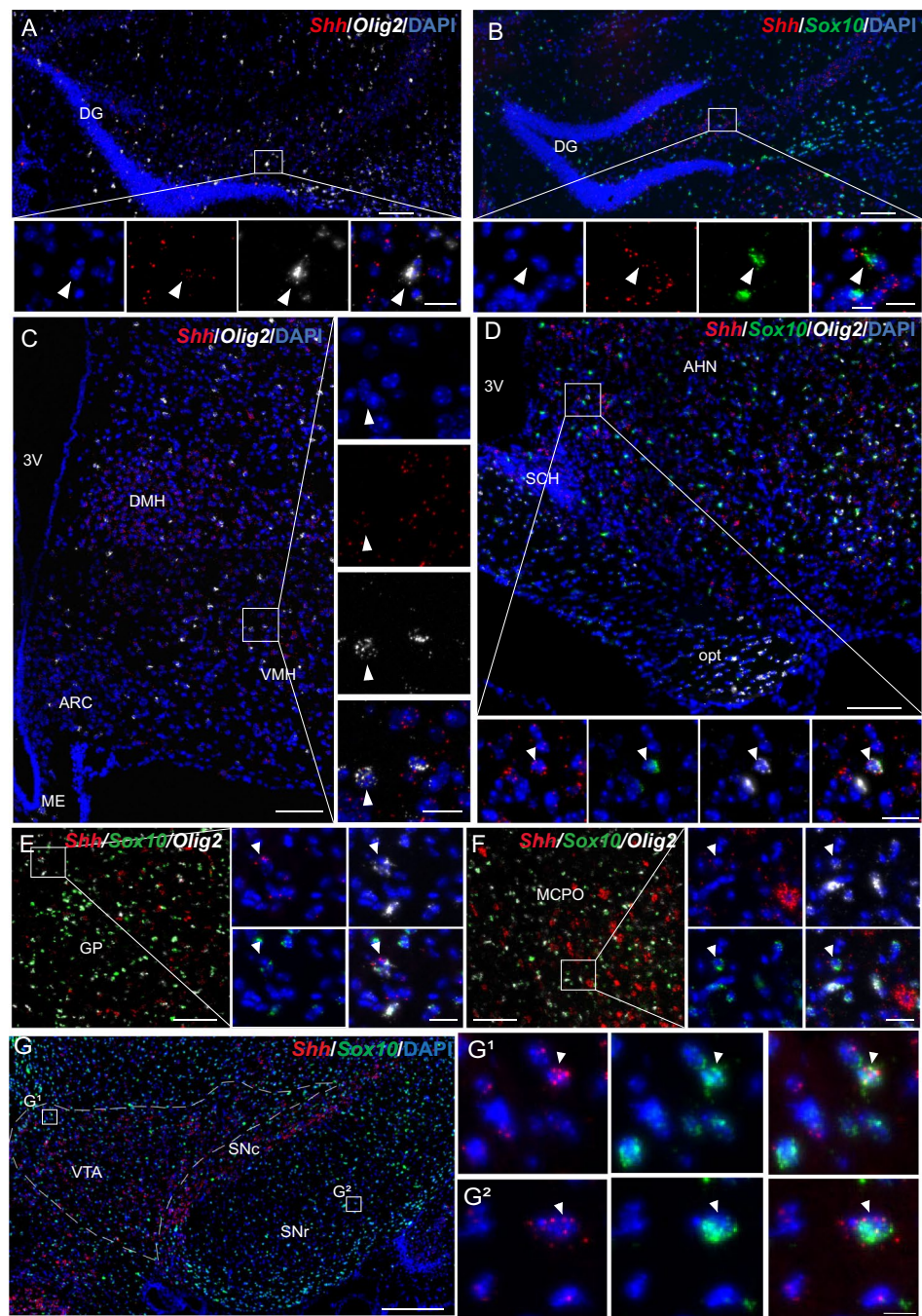
of single labeled cells in the arcuate (ARC), ventromedial (VMH) and dorsomedial (DMH) hypothalamic nuclei, represented by plate 70 of the Allen Adult Mouse Brain Atlas, and in the substantia nigra compacta (SNc) and ventral tegmental area (VTA), represented by plate 82 of the same Atlas. Cells were counted unilaterally in the ARC, VMH, DMH, SNc and VTA delimited by DAPI nuclear staining from the analysis of one section per adult mouse, *N* = 3 animals. Between 100 and 170 cells were counted as TH-expressing neurons in the SNc and VTA nuclei. From 100 to 400 HuC/D-expressing cells were counted in the ARC, VMH, and DMH. Between 100 and 200 cells were counted as *Gad67*-expressing neurons in the ARC and DMH; while from 9 to 18 *Gad67*-expressing neurons were counted in the VMH, where *Gad67* transcript is less expressed. From 100 to 225 *nNOS*-expressing cells were counted in the VMH and DMH; while 42–48 cells were counted in the ARC where the *nNOS* transcript is less expressed. Density of *Shh* mRNA was estimated by RNAscope from one section per adult mouse, *N* = 3 animals, and scored as follows: 4⁺: very high density, > 30 dots/cell; 3⁺: high density, 10–30 dots/cell; 2⁺: moderate density, 6–9 dots/cell; 1⁺: low density, 2–5 dots/cell; 0⁺: undetectable, 0–1 dot/cell. Counting of colocalized staining was undertaken using ROI and multi-point ImageJ tools. Data are represented as the mean ± SEM.

Results

Shh mRNA expression is widespread in the brain, whereas *Dhh* and *Ihh* mRNAs are not

We used single-molecule multiplex fluorescent in situ hybridization (smFISH) to study the distribution of *Shh*, *Dhh*, and *Ihh* mRNAs in the adult mouse brain (Fig. 1). We successfully detected consistent and reproducible expression of *Shh* transcripts using RNAscope in various brain regions (Fig. 1A–C). As shown in Table 1, the cell-associated density of *Shh* mRNA was assessed from the number of spots counted per nucleus and classified as "very high density," "high density," "moderate density," "low density," and "undetectable." Regions expressing very high density of *Shh* signals were found in the striatum, pallidum, claustrum, trigeminal mesencephalic and motor nuclei, facial nucleus, and in the Purkinje cell layer of the cerebellum, as previously reported using a digoxigenin-labeled *Shh*-specific cRNA probe (Traiffort et al. 1998, 1999, 2001). However, most brain regions had cells expressing *Shh* mRNA at low to moderate or low to high density, whereas fibrous tracts and a few nuclei expressed cells at low density only (Table 1). Probes for *Dhh* and *Ihh*, the other two members of the Hedgehog (Hh) family (Briscoe and Therond 2013) did not generate significant signals in adjacent brain

Fig. 3 Representative images of multiplex fluorescent in situ hybridization of *Shh* (red) with the oligodendroglial markers *Sox10* (green) and *Olig2* (white) in the mouse hippocampus (A, B), hypothalamus (C, D), in the globus pallidus (GP) (E) and the magnocellular preoptic nucleus (MCPO) (F) of the pallidum, and in the midbrain (G). *Shh* is detected in *Sox10* or *Olig2* positive cells scattered in these brain regions as shown in the ventromedial hypothalamic nucleus (VMH) (C), the sub-paraventricular zone above the anterior suprachiasmatic nucleus (SCH) of the hypothalamus (D), and the ventral tegmental area (VTA) and the substantia nigra pars reticulata (SNr) (G1–G2). Arrowheads show *Shh* positive cells represented in single and merged channels with the nuclear marker DAPI (blue). White squares are magnified below the main panel (A, B, D) and on the side of the main panel (C, E–G). DG dentate gyrus of the hippocampus, 3V third ventricle, ME median eminence, ARC arcuate hypothalamic nucleus, DMH dorsomedial hypothalamic nucleus, opt optic chiasma, AHN anterior hypothalamic nucleus, SNc substantia nigra pars compacta. Scale bars: A–F = 100 μ m; G = 200 μ m; G1–G2 = 10 μ m; all magnifications 20 μ m



sections by RNAscope: one dot per nucleus was occasionally observed with both probes as shown in the cerebral cortex, hippocampus, and in the tuberal region of the hypothalamus (Fig. 1D–I).

Shh mRNA is present in cells expressing neuronal and oligodendroglial markers

Further phenotyping of *Shh* mRNA-expressing cells in the mouse brain indicated that most of these cells were positive

for the neuronal marker HuC/D, as shown in the cerebral cortex (Fig. 2A, B), the hippocampus (Fig. 2C) and the tuberal region of the hypothalamus (Fig. 2D), and recapitulated in Table 2. In the cortex and hypothalamus, activation of *Shh* signaling results in a different modulation of Gli1-3 in astrocytes (Tirou et al. 2021). Detailed analysis of *Shh* mRNA expression in HuC/D-positive cells revealed that in the hypothalamus, $34.0 \pm 3.2\%$ of neurons were positive for *Shh* transcripts in the ARC, $72.8 \pm 4.3\%$ in the VMH, and $42.5 \pm 0.3\%$ in the DMH (Fig. 2E, Table 3); whereas

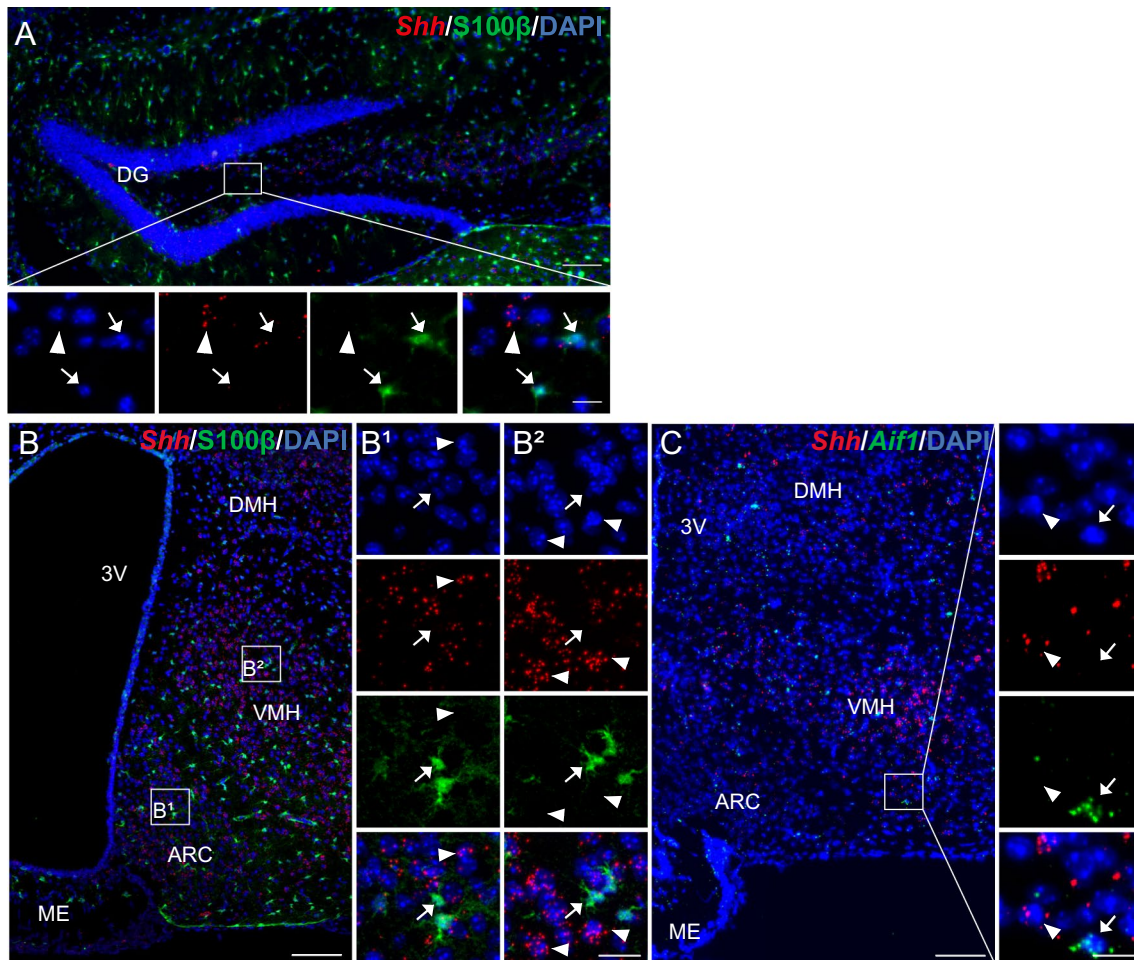


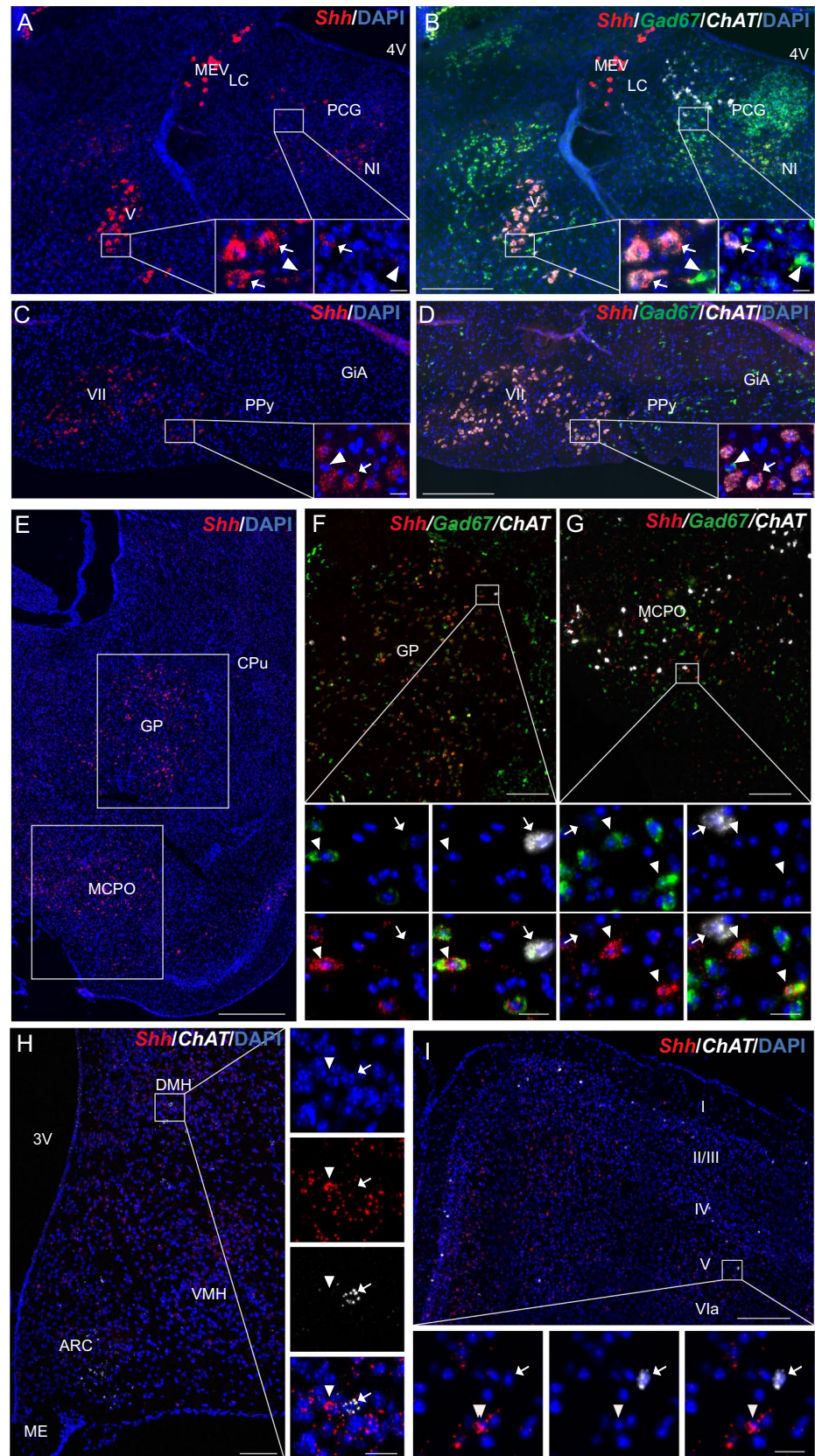
Fig. 4 Representative images of multiplex fluorescent in situ hybridization of *Shh* (red) combined with immunofluorescence with the S100 β astrocytic marker (green) (**A**, **B**) or with in situ hybridization with the *Aif1* microglia marker (green) (**C**) in the mouse hippocampus (**A**) and hypothalamus (**B**, **C**). *Shh* transcripts are not detected in S100 β ⁺ astrocytes as shown in the arcuate hypothalamic nucleus (ARC) (**B1**) and in the ventromedial hypothalamic nucleus (VMH) (**B2**), nor in *Aif1*⁺ microglia (**C**). Arrowheads show *Shh* positive cells

and arrows show S100 β ⁺ or *Aif1*⁺ cells. B1 and B2 are magnifications of white boxes in **B**. White squares are magnified below the main panel (**A**) and on the side of the main panel (**C**) in merge and single channel with the nuclear marker DAPI (blue). *DG* dentate gyrus of the hippocampus, *3V* third ventricle, *DMH* dorsomedial hypothalamic nucleus, *ARC* arcuate hypothalamic nucleus, *ME* mammillary epithelium. Scale bars: **A–C** = 100 μ m; **B1–B2** = 20 μ m; all magnifications = 20 μ m

in the cerebral cortex, 29.6 \pm 3.3% of the neurons (Table 3) expressed *Shh* mRNA. In the hypothalamus, *Shh* mRNA density was moderate to high in 4%–6% of ARC and DMH HuC/D-positive neurons and in 25% of VMH neurons (Fig. 2E). We also identified high *Shh* mRNA expression in GABAergic, cholinergic, nitroergic, and dopaminergic cells, as shown below and summarized in Tables 2 and 3. In the cerebral cortex, 95 \pm 0.5% of the cells expressing *Shh* mRNA were HuC/D neurons (data not shown). *Shh* mRNA was also identified in a restricted cell population expressing the oligodendroglial markers *Sox10* or/and *Olig2* in all brain regions, as shown in the hippocampus (Fig. 3A, B) and in hypothalamic regions (Fig. 3C, D), in the globus

pallidus and preoptic area (Fig. 3E, F), and in the dopaminergic region of the midbrain, including the ventral tegmental area (VTA), substantia nigra pars compacta (SNc) and reticulata (SNr) (Fig. 3G). *Shh* mRNA was undetectable in cells expressing the astroglial marker S100 β as shown in the hippocampus (Fig. 4A) and in the tuberal region of the hypothalamus (Fig. 4B). Characterization of the microglial marker *Aif1* by smFISH on adult mouse brain sections revealed intense signals associated with scattered nuclei in brain regions, as shown in hypothalamic nuclei (Fig. 4C), in agreement with the distribution of IBA1-positive microglial cells (Lier et al. 2021). *Shh* mRNA was not identified in microglial cells expressing *Aif1* transcripts, as shown in the hypothalamus (Fig. 4C).

Fig. 5 Representative images of multiplex fluorescent in situ hybridization of *Shh* (red) with the neuronal markers *Gad67* (green) and *ChAT* (white), together or alone, in the mouse hindbrain (A–D), the pallidum and the preoptic region (E–G), the tuberal region of the hypothalamus (H) and the cortex (I). *Shh* transcripts show wide expression with very high density level in *ChAT*⁺ cholinergic neurons (arrows) in the motor trigeminal nucleus (V), the pontine central gray (PCG) (B) and facial nucleus (VII) (D), while its intensity is lower in *Gad67*-expressing cells in those nuclei (arrowheads) (B, D). *Shh* transcripts show very high density level also in the globus pallidus (GP), the magnocellular preoptic nucleus (MCPO) and the dorsal part of the anterior amygdala area (AAD) (E). *Shh* is visualized at high levels in *Gad67*-expressing GABAergic neurons (arrowheads) but not cholinergic neurons expressing *ChAT* (arrows) in the GP, MCPO and AAD (F, G). *Shh* expression is very low in *ChAT*⁺ cholinergic neurons of the basal nuclei of the tuberal region of the hypothalamus, as shown in the dorsomedial hypothalamic nuclei (DMH) (H), while it is absent in *ChAT*⁺ cortical neurons (I). Arrowheads show *Shh*-expressing cells, while arrows show *ChAT*-expressing neurons (H, I). White squares are magnified on the corner of the main panel (A–D), below the main panel (F, G, I), or on the side (H), in merge and single channel with the nuclear marker DAPI (blue). *MEV* trigeminal nucleus, *4V* fourth ventricle, *LC* locus ceruleus, *NI* nucleus incertus, *PPy* parapyramidal nucleus, *GiA* anterior gigantocellular nucleus, *CPu* caudate putamen, *ARC* arcuate hypothalamic nucleus, *3V* third ventricle, *ME* median eminence. Scale bars: A–D, I = 200 μ m; E = 500 μ m; F–H = 100 μ m; all magnifications = 20 μ m



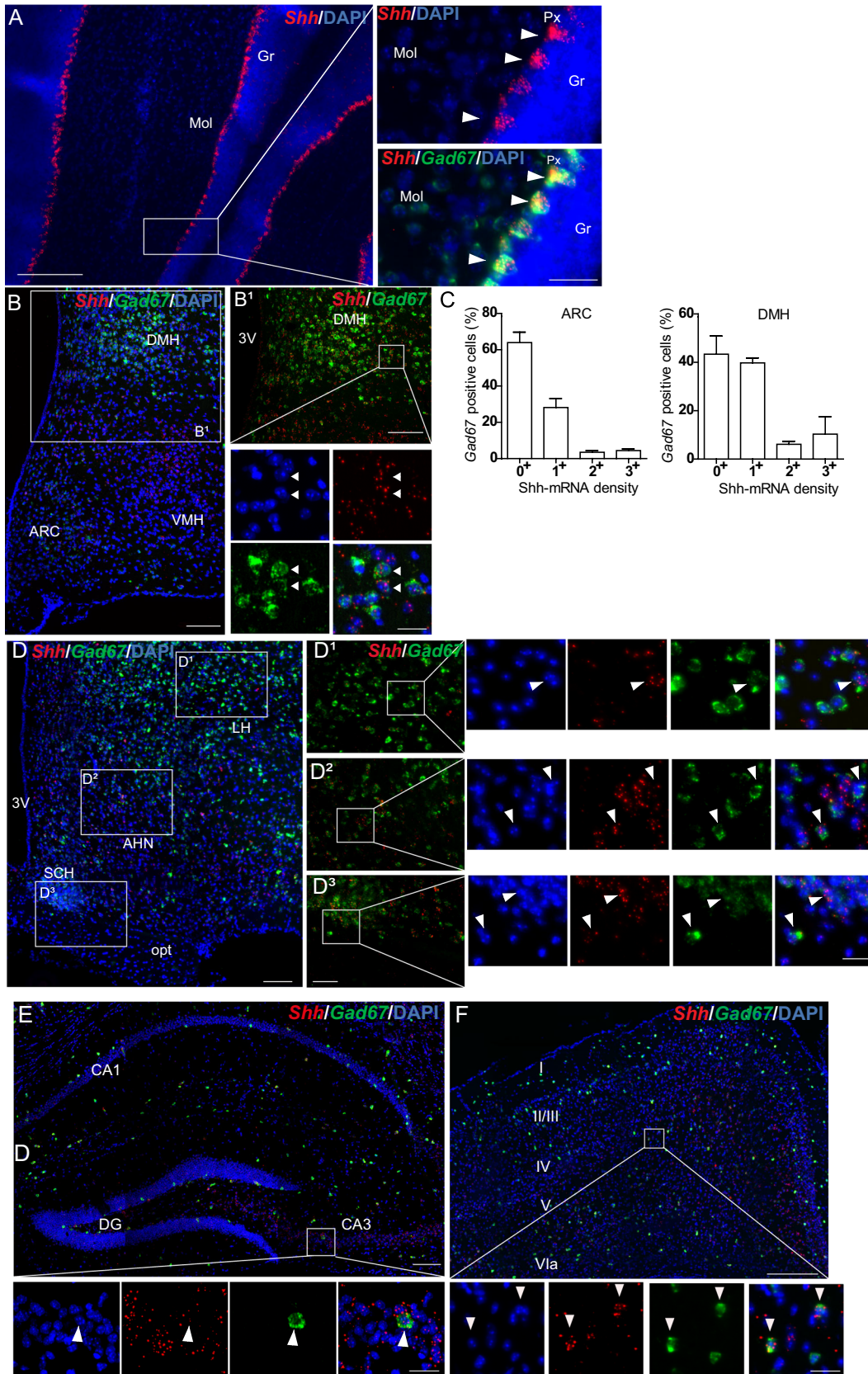


Fig. 6 Representative images of multiplex fluorescent in situ hybridization of *Shh* (red) with the neuronal markers *Gad67* (green) in the mouse cerebellum (A), the tuberal region and the anterior region of the hypothalamus (B–B¹, D–D³), the hippocampus (E) and the cerebral cortical layers (F). High level of *Shh* transcripts is detected in Purkinje cells (Px) expressing *Gad67* (A). In the hypothalamus (B), *Shh* transcripts show various density levels in *Gad67* GABAergic neurons as shown in the dorsomedial hypothalamic nucleus (DMH) (B1), and as quantified in the arcuate hypothalamic nucleus (ARC) and the DMH (C). Mean ± SEM. Density of *Shh* mRNA was estimated by RNAscope from *N*=3 animals. *Shh* transcripts are also widely distributed in *Gad67*-expressing GABAergic neurons in the lateral hypothalamus (LH) (D1), the anterior hypothalamic nucleus (AHN) (D2), and in the suprachiasmatic nucleus (SCH), showing a less dense distribution at the level of the optic tract (D3). D1–D3 are magnifications of boxed areas in D. In the hippocampus (E) and in the cortex (F), some *Shh*-expressing cells are scattered GABAergic neurons expressing *Gad67* as shown in the CA3 pyramidal cell layer (E) and in the cerebral cortical layer V (F). Arrowheads show *Shh* and *Gad67* double positive cells represented in merge and single channel with the nuclear marker DAPI (blue). White boxes are magnified on the side of the main panel for A–D3, and below the main panel for (E, F). *Mol* molecular layer, *Gr* granular layer, *3V* third ventricle, *VMH* ventromedial hypothalamic nucleus, *DG* dentate gyrus. Scale bars: A = 200 μm; B–B1, D–D3, E, F = 100 μm; magnifications = 50 μm (A) and 20 μm (B1, D1–D3, E, F)

Shh mRNA is expressed in ChAT cholinergic neurons

Shh mRNA expression in *ChAT*-expressing neurons in the adult mouse brain is shown in Table 2. *Shh* smFISH associated with the neuronal marker *ChAT* revealed a very high density of *Shh* transcripts in *ChAT*-positive cholinergic neurons located in the trigeminal mesencephalic and motor nuclei and in the facial nucleus (Fig. 5A–D), consistent with their expression in motor neurons, as previously reported (Traiffort et al. 1998, 1999, 2001). In addition, a moderate to high density distribution of *Shh* mRNA was observed in cholinergic neurons scattered in the pontine central gray (Fig. 5A, B), in the magnocellular preoptic nucleus of the pallidum (Fig. 5E, G; Table 2). *Shh* transcripts were also distributed at low density in *ChAT*-positive neurons located in hypothalamic nuclei, including the ARC, dorsomedial, and central parts of the VMH, DMH, and posterior hypothalamic nucleus (Fig. 5H; Table 2). *Shh* transcripts were undetectable in cholinergic neurons distributed in different layers of the cerebral cortex (Fig. 5I), in the caudate putamen and globus pallidus (Fig. 5F), or in the posterior part of the lateral hypothalamic nucleus or tuberal nucleus (Table 2).

Shh mRNA is expressed in Gad67 GABAergic neurons

The expression of *Shh* mRNA in *Gad67* GABAergic neurons in the adult mouse brain is reported in Table 2. Very high density of *Shh* transcripts in *Gad67*-expressing cells was observed in the pallidum (Fig. 5E–G) and in

the Purkinje cell layer of the cerebellum in agreement with their expression in Purkinje cells (Fig. 6A). A high number of *Shh*⁺*Gad67*⁺ neurons were identified in the globus pallidus and the adjacent magnocellular preoptic nucleus (Fig. 5E–G), whereas a more limited number was present in hypothalamic nuclei such as in the ARC, the VMH and the DMH (Fig. 6B) and in more anterior hypothalamic nuclei (Fig. 6D). Moderate to high density of *Shh* mRNA was also identified in scattered GABAergic neurons located in the CA1–CA3 pyramidal cell layers of the hippocampus (Fig. 6E), in the polymorph and molecular layer of the dentate gyrus, and in layers II/III, V, VIa and VIb of the cerebral cortex (Fig. 6F), in the caudate putamen (Fig. 5E–G), in the pontine central gray (Fig. 5B), in the motor trigeminal and facial nuclei, and also in the intermediate and gigantocellular reticular nuclei (Fig. 5D). Low density of *Shh* mRNA was also detected in *Gad67*⁺ cells located throughout brain regions (Figs. 5A–D, 6B, D–F and Table 2). Quantification of *Shh* mRNA expression indicated that 36 ± 6% of GABAergic neurons were *Shh*⁺ in the ARC and 56 ± 7% in the DMH (Fig. 6C; Table 3); while in the cerebral cortex 6 ± 1% of *Gad67*⁺ neurons were expressing *Shh* transcripts (Table 3), with a total of 24 ± 3% of the cells expressing *Shh* mRNA being *Gad67*⁺ GABAergic neurons (data not shown). *Shh* mRNA was also evidenced in *Gad67*⁺ neurons in the VMH (Table 2) that occasionally populate this nucleus (Hrabovszky et al. 2012).

Shh mRNA is expressed in nNOS nitrenergic neurons

Shh mRNA expression in *nNOS*-expressing neurons in the adult mouse brain is shown in Table 2. *Shh* smFISH combined with the *nNOS* marker identified consistent and robust expression of *Shh* mRNA in nitrenergic neurons located in different brain areas. A moderate to high density of *Shh* transcripts was observed in cells located in the mesencephalic trigeminal nucleus and pontine central gray (Fig. 7A, B), in the intermediate reticular and gigantocellular nuclei, and in the facial nucleus in the medulla (Fig. 7C–E), in the CA3 pyramidal cell layer of the hippocampus, suggesting their expression in pyramidal neurons (Fig. 8A, A2), in various hypothalamic nuclei such as the ARC, VMH, DMH (Fig. 8B, C) and the posterior part of the lateral hypothalamic nucleus, and in cortical layers II/III, V, and VIa (Fig. 9A–A1). In the above regions, a low density of *Shh* mRNA was also detected in scattered cells expressing *nNOS*. We also identified a low density of *Shh* transcripts in nitrenergic cells in hippocampal sparse cells located in the CA1 and CA2 pyramidal cell layers and in the dentate gyrus (Fig. 8A–A1), in the molecular layer of the cerebellum (Fig. 9B–D), in the tuberal and posterior hypothalamic nuclei of the hypothalamus (Fig. 8B–C), and in layers I, IV, and VIb of the cerebral cortex (Fig. 9A, A2). Quantification of *Shh*

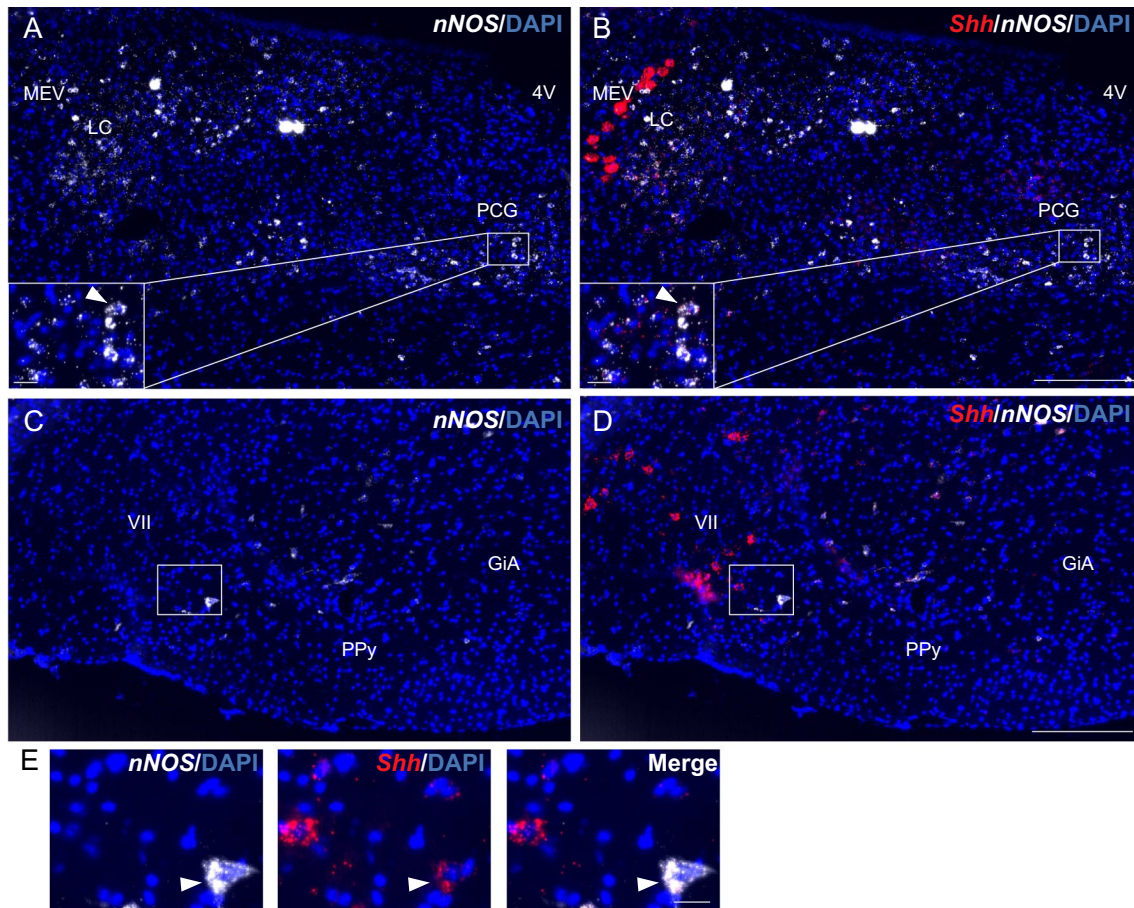


Fig. 7 Representative images of multiplex fluorescent in situ hybridization of *Shh* (red) with the neuronal marker *nNOS* (white) in the mouse hindbrain. *Shh* transcripts are evidenced in cells expressing *nNOS* in the PCG (A, B) and in the facial nucleus (VII) (C–E) (arrowheads). E is a magnification of boxed areas in C, D. White

squares are magnified on the corner of the main panels for A, B. Sections are counterstained using DAPI to visualize cell nuclei. 4V fourth ventricle, MEV trigeminal nucleus, LC locus ceruleus, PPy parapyramidal nucleus, GiA anterior gigantocellular nucleus. Scale bars: A–D=200 μ m; all magnifications=20 μ m

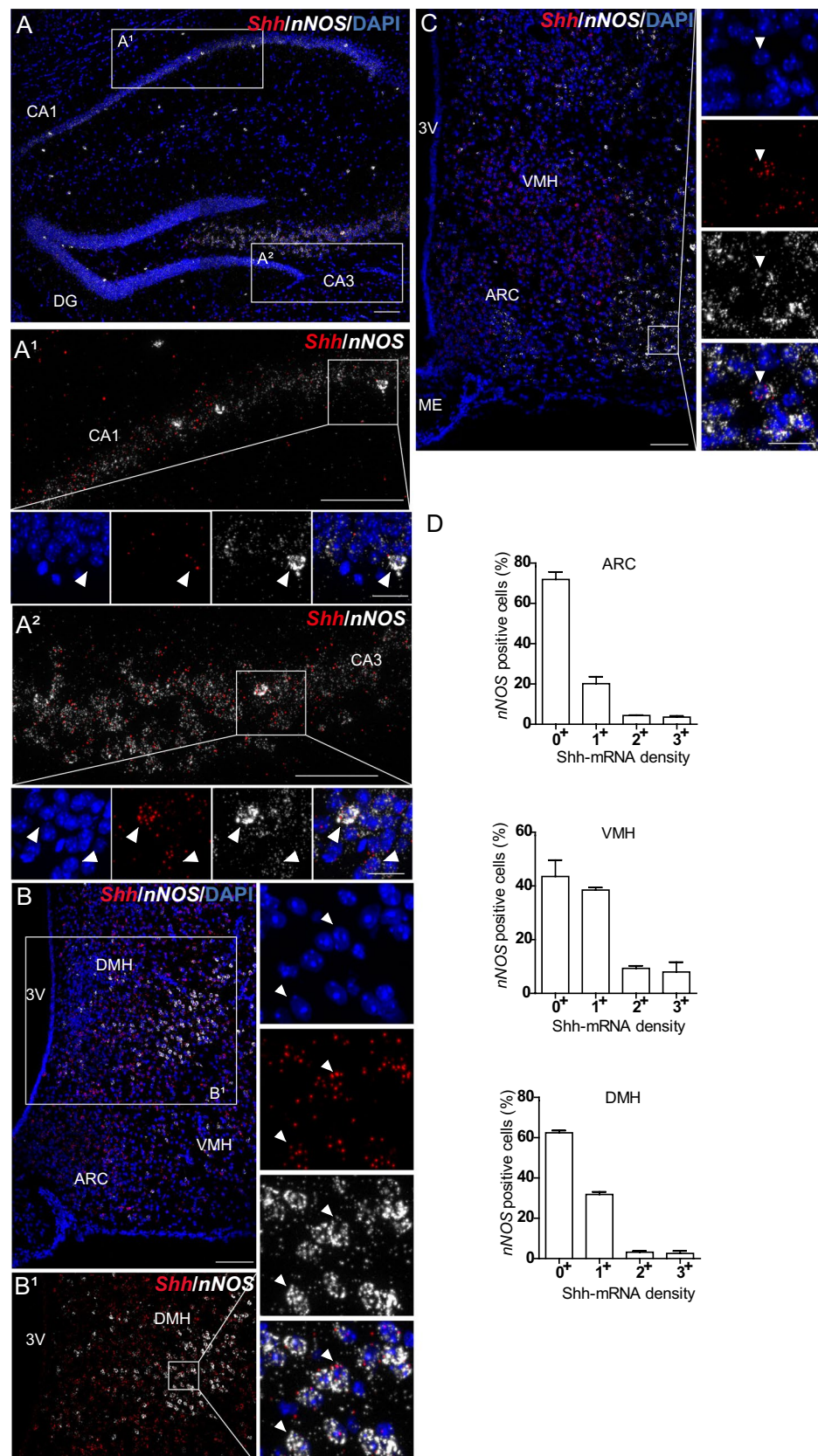
mRNA expression indicates that $28 \pm 4\%$ of nitroergic neurons are *Shh*⁺ in the ARC, $56 \pm 6\%$ in the VMH, and $38 \pm 1\%$ in the DMH (Fig. 8D; Table 3). In the cerebral cortex $1.8 \pm 0.2\%$ of *nNOS*⁺ neurons are *Shh*⁺ (Table 3) with a total of $6 \pm 1.5\%$ of the cells expressing *Shh* mRNA being *nNOS*⁺ nitroergic neurons.

Shh mRNA is expressed in tyrosine hydroxylase-expressing dopaminergic neurons

Shh mRNA expression in the hindbrain dopaminergic neurons is shown in Table 2. *Shh* smFISH combined with immunofluorescence of the neuronal tyrosine hydroxylase (TH) marker revealed a broad distribution of *Shh* mRNA in dopaminergic neurons in both the VTA and SNc (Fig. 10A, C), in agreement with a previous report

based on a reporter mouse line (Gonzalez-Reyes et al. 2012; Turcato et al. 2022). Detailed analysis indicated that almost all TH-positive neurons expressed *Shh* transcripts at low to high density in the VTA ($98 \pm 6\%$) and in the SNc ($97 \pm 4\%$). Interestingly, a large proportion of TH-positive dopaminergic neurons expressed a high density of *Shh* mRNA ($44 \pm 6\%$ in the VTA and $40 \pm 3\%$ in the SNc) (Fig. 10A, C–E). *Shh* smFISH combined with *Ptc* revealed co-expression of the *Shh* receptor with *Shh* in TH-positive neurons. However, the highest expression of *Ptc* was identified in scattered cells surrounding TH neurons in both the VTA and the SNc (Fig. 10A–D). SmFISH of *Ptc* and *Smo*, combined with immunofluorescence of the astroglial marker S100 β , revealed that these cells were astrocytes and also expressed the Hh signaling pathway transducer *Smo* (Fig. 10F–I).

Fig. 8 Representative images of multiplex fluorescent in situ hybridization of *Shh* (red) with the neuronal marker *nNOS* (white) in the mouse hippocampus and the tuberal region of the hypothalamus (A–C). *Shh* transcripts are detected at different intensity levels in nitroergic neurons expressing *nNOS* as shown in the CA1 (A1) and the CA3 (A2) pyramidal cells layers, respectively, with most of CA3 pyramidal cells expressing both *Shh* and *nNOS* transcripts (A2). *Shh* transcripts are widely distributed at different intensity levels in nitroergic neurons expressing *nNOS* located in the arcuate hypothalamic nucleus (ARC), the ventromedial hypothalamic nucleus (VMH) and the dorsomedial hypothalamic nucleus (DMH) (B, C). Arrowheads show *Shh* and *nNOS* double positive cells. White square are magnified below the main panel for B1–C. Percentage of *nNOS*⁺ (F) neurons expressing different level of *Shh* mRNA density was quantified in the ARC, the VMH and the DMH. Mean \pm SEM. Density of *Shh* mRNA was estimated by RNAscope from $N = 3$ animals. DG dentate gyrus, 3V third ventricle, ME median eminence. Scale bars: A, B–B1, C = 100 μ m; A1–A2 = 50 μ m; all magnifications = 20 μ m



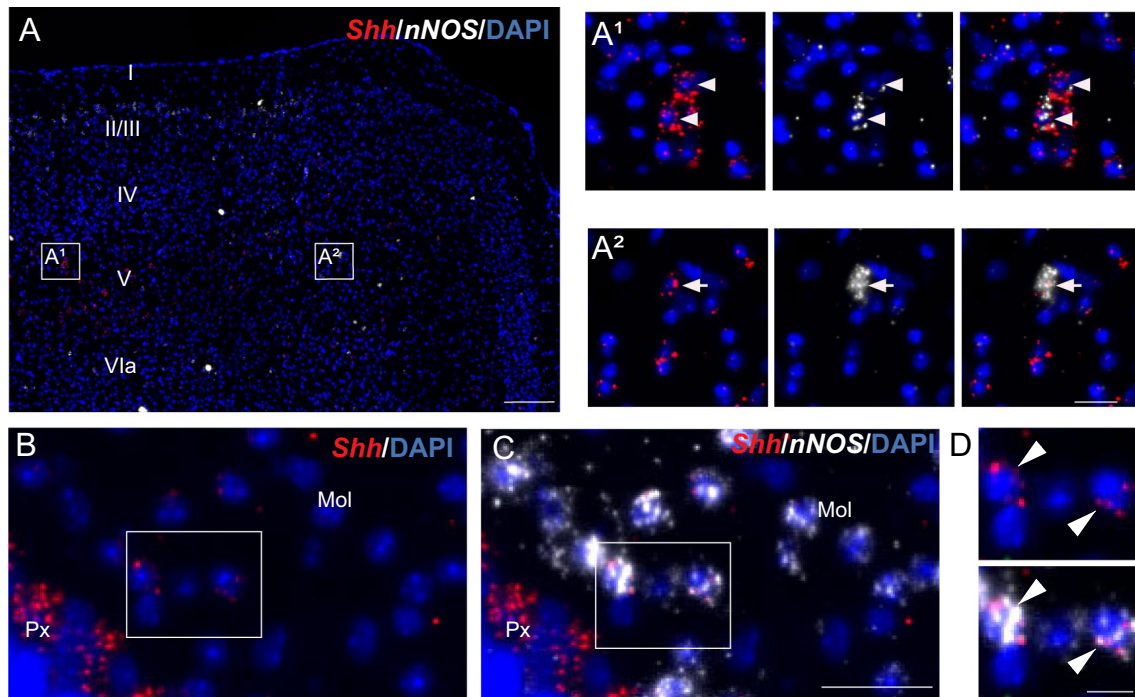


Fig. 9 Representative images of multiplex fluorescent in situ hybridization of *Shh* (red) with the neuronal marker *nNOS* (white) in the mouse cerebral cortical layers (A) and the cerebellum (B–D). In all cerebral cortical layers, *Shh* intensity level is high in cells expressing a low intensity for *nNOS* transcripts (A1) (arrowheads), while it is low in cells expressing a high intensity level for *nNOS* transcripts (A2) (arrow). In the molecular layer of the cerebellum, *Shh* is distrib-

uted with a lower intensity level in nitrergic neurons expressing *nNOS* (B–D) (arrowheads). D is a magnification of boxed areas in B and C. White squares are magnified on the side of the main panels in merged channels with the nuclear marker DAPI (blue). Mol molecular layer, Px Purkinje cell layer. Scale bars: A = 200 μ m; B, C = 30 μ m; magnifications = 20 μ m (A) and 10 μ m (B, C)

Discussion

Here, by further exploring the brain distribution of *Shh*, *Dhh*, and *Ihh* transcripts using smFISH (Tirou et al. 2020), we identified much broader expression of *Shh* mRNA than originally reported; whereas, *Dhh* and *Ihh* signals were not detectable (see summary Fig. 11A–D). Our current data unequivocally identify *Shh* transcripts in various populations of neurons as well as in a restricted population of oligodendroglial cells, both distributed in almost all brain regions. Astrocytes have been proposed as the major *Shh*-responsive cells in the adult rodent brain (Garcia et al. 2010, 2018; Ruat et al. 2015; Allahyari et al. 2019; Hill et al. 2019; Tirou et al. 2021; Wang et al. 2021). Thus, *Shh* synthesized and released by these neuronal and oligodendroglial cells is expected to regulate Hh signaling in astrocytes in these regions. We unequivocally identified *Shh* mRNA in GABAergic (*Gad67*⁺), cholinergic (*ChAT*⁺), nitrergic (*nNOS*⁺), and dopaminergic (TH⁺) neurons, and suggest its expression in other populations of neurons, including glutamatergic neurons in the cerebral cortex and

in hypothalamic nuclei. These results are in agreement with previous reports describing *Shh*-transcript expression in GABAergic, cholinergic, dopaminergic, and some glutamatergic neurons using digoxigenin-labeled riboprobes (Traiffort et al. 1998; Traiffort et al. 2001; Charytoniuk et al. 2002; Lai et al. 2003; Machold et al. 2003; Loulier et al. 2006; Angot et al. 2008; Desouza et al. 2011; Ihrle et al. 2011; Ferent et al. 2013a; Eitan et al. 2016; Sanchez and Armstrong 2018; Sanchez et al. 2018; Gonzalez-Reyes et al. 2019; Rivell et al. 2019) or reporter lines (Garcia et al. 2010; Ihrle et al. 2011; Sanchez et al. 2018). Our present work identifies for the first time to our knowledge, *Shh* expression in *nNOS* neurons in several brain regions including the cerebral cortex, hippocampus and hypothalamus. Interestingly, neuronal *Shh* expression occurs at different levels of intensity, suggesting that *Shh* signals are tightly regulated in these cells. We also extend our previous observation of oligodendroglial *Shh* by reporting the presence of *Shh* mRNA in cells expressing the oligodendroglial markers *Sox10* or/and *Olig2* in all brain regions.

nNOS is responsible for the production of the radical gas nitric oxide (NO), which can act as an autocrine or

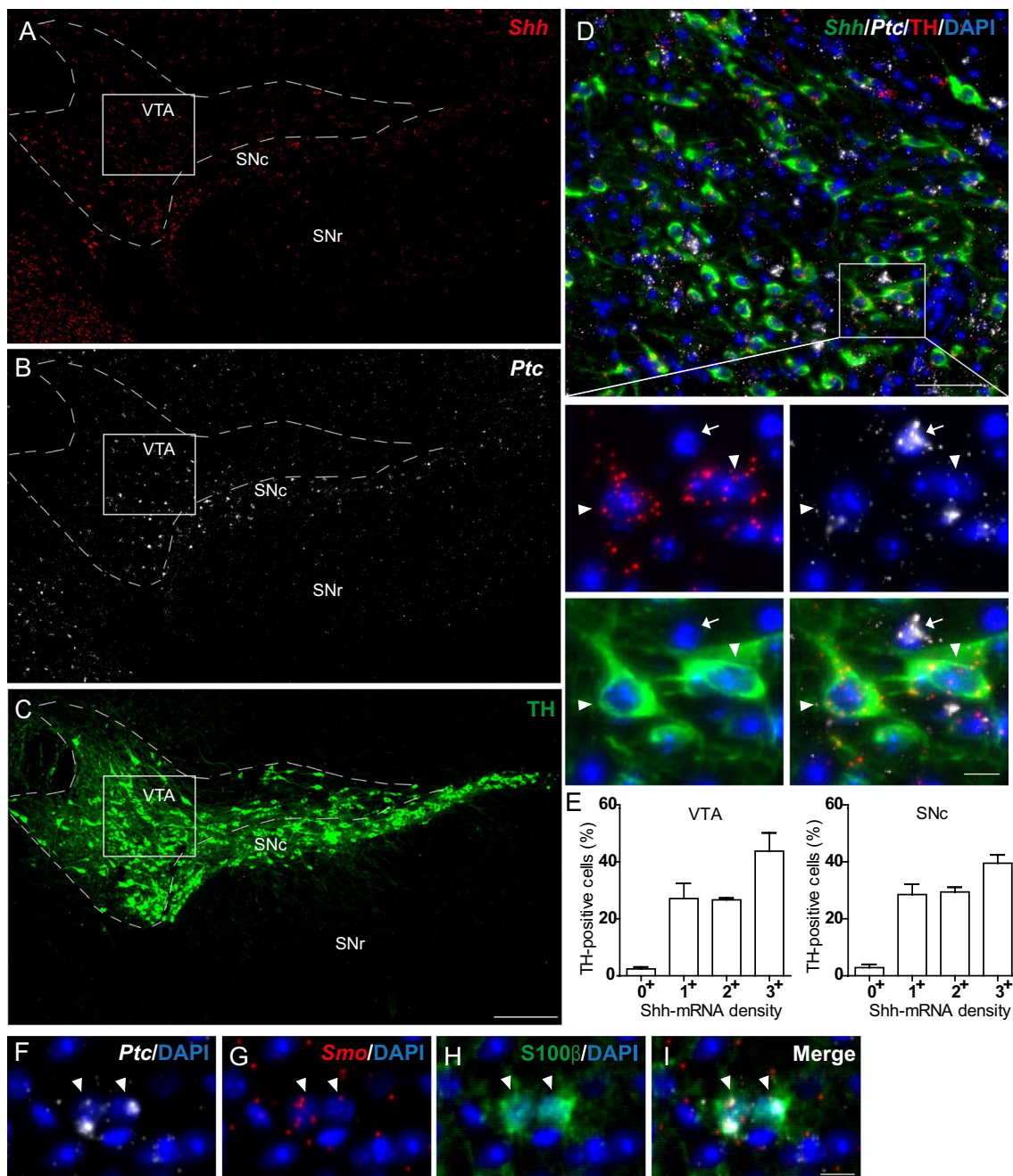
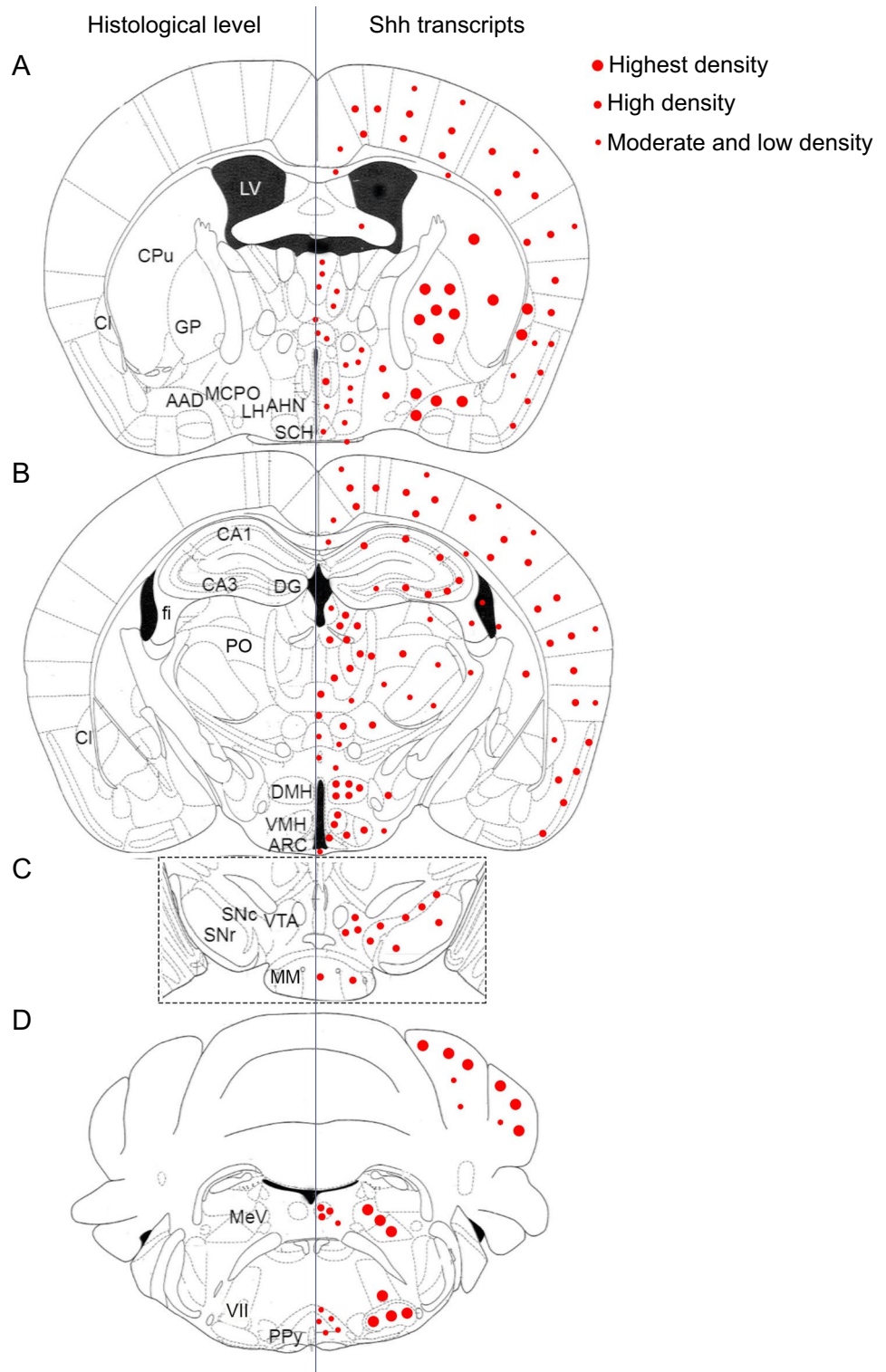


Fig. 10 Representative images of fluorescent in situ hybridization of *Shh* (red) combined with immunofluorescence for the dopaminergic marker tyrosine hydroxylase (TH) (green), or with in situ hybridization of its receptor *Ptc* (white), in the mouse midbrain. *Shh* and its receptor *Ptc* transcripts are widely distributed in the ventral tegmental area (VTA), delimited by the white dashed line, the substantia nigra pars compacta (SNc) and the substantia nigra pars reticulata (SNr) (A, B). Dopaminergic neurons, identified through TH-immunolabelling, are localized in the VTA and the SNc but not in the SNr (C). *Shh* transcripts are detected with different intensity levels in TH-expressing neurons (arrowheads), while *Ptc* transcripts are low in TH⁺ cells and higher in TH⁻ cells (arrows), as exemplified in the VTA (D). D is the magnification of the boxed area in A–C. Percent-

age of TH⁺ neurons expressing different level of *Shh* mRNA density was quantified in the VTA and SNc. Mean \pm SEM. Density of *Shh* mRNA was estimated by RNAscope from $N=3$ animals. More than 100 TH-expressing cells were counted per animal in each of the two regions analyzed (E). Astrocytes labeled by the astrocytic marker S100 β (green) express both *Ptc* and the transducer of the Hh signaling pathway *Smo* (red) detected by fluorescent in situ hybridization, as indicated by arrowheads in a magnification of the SNc (F–I). Sections were counterstained with DAPI (blue) to visualize cell nuclei and identify the morphological limits of each structure. Scale bars: A–C = 200 μ m; D = 50 μ m; F–I and all magnifications = 10 μ m

Fig. 11 Line drawings of coronal sections of the adult mouse brain illustrating the distributions of *Shh* transcripts, indicated by red dots. These data are derived from ISH experiments conducted with *Shh* probe as described in Figs. 1, 2, 3, 4, 5, 6, 7, 8, 9, 10 and Table 1. The left column illustrates the histological level of neuroanatomical structures. VII, facial nucleus, *AAD* anterior amygdala area, dorsal, *AHN* anterior hypothalamic nucleus, *ARC* arcuate hypothalamic nucleus, *Cl* claustrum, *CPu* caudate putamen, *DG* dentate gyrus, *DMH* dorsomedial hypothalamic nucleus, *fi* fimbria, *GP* globus pallidus, *LH* lateral hypothalamic nucleus, *LV* lateral ventricle, *MCPO* magnocellular preoptic nucleus, *MeV* mesencephalic trigeminal nucleus, *MM* mammillary body, *PO* posterior thalamic nucleus, *PPy* parapyramidal nucleus, *SCH* suprachiasmatic nucleus, *SNc* substantia nigra pars compacta, *SNr* substantia nigra pars reticulata, *VMH* ventromedial hypothalamic nucleus, *VTA* ventral tegmental area. Bregma levels (mm): **A**, -0.46 ; **B**, -1.70 ; **C** -3.08 ; **D**, -5.68



paracrine messenger. Among the transduction pathways triggered by NO, activation of guanylate cyclase initiates transcription of various genes involved in multiple physiological processes, including modulation of synaptic transmission. A link between Shh signaling and NO has been established by a series of observations reporting that cGMP analogs increase the Shh differentiation response on chick neuronal explants (Robertson et al. 2001) while reduced NO levels in immature granule cell precursors (GCPs) of the outer granule cell layer during postnatal cerebellar development increase Ptc expression and impair GCP migration (Haag et al. 2012). The expression of Hedgehog-interacting protein (Hip), a negative regulator of Shh, in nNOS-positive neurons in the rodent brain (Loulier et al. 2005) also argues for a close regulation between NO and Shh signals. The presence of Shh transcripts in nNOS neurons suggests that, in these cells, Shh signals may be under the control of nNOS activity. Interestingly, the interaction of nNOS with Sox2 in the nucleus has been proposed to promote neuronal Shh transcription and to protect neurons from glutamate-induced excitotoxicity (Zhang et al. 2016). Alternatively, Shh may regulate nNOS activity through its action on local astrocytic Hh signaling and the release of glutamate and ATP factors, as demonstrated in cerebellar astrocytes (Okuda et al. 2016). Whether NO controls Shh transcription, synthesis, secretion, or degradation and whether Shh production attenuates or exacerbates the neurotoxicity associated with excessive NO production deserves further investigation.

In cerebral cortical layers, nNOS neurons have been divided into two types of inhibitory GABAergic neurons based on the intensity of nNOS immunoreactivity and NADPH diaphorase staining. Type I cells express high levels of nNOS immunoreactivity and NADPH diaphorase activity, are mainly found in layers V and VI (Oermann et al. 1999; Vercelli et al. 2000; Wiencken and Casagrande 2000; Barbosa et al. 2001; Lee and Jeon 2005; Perrenoud et al. 2012) and correspond mainly to projection neurons activated during sleep (Gerashchenko et al. 2008; Tricoire and Vitalis 2012). In our study, they may correspond to cells that express the highest level of nNOS mRNA and express little Shh mRNA (Fig. 9A, A2).

Type II cells correspond to a more heterogeneous population of neurons distributed throughout the mouse cortical layers, exhibiting low nNOS immunoreactivity and diaphorase activity (Lee and Jeon 2005; Perrenoud et al. 2012). They classically correspond to small- to medium-sized neurons with less characterized functions and also include neurogliaform interneurons mediating inhibitory GABAergic effects on pyramidal cells (Karagiannis et al. 2009; Olah et al. 2009). In our study, type II cells may correspond to cells expressing a lower level of nNOS mRNA (Fig. 9A,

A1). Interestingly, the intensity of Shh mRNA is low to high in these cells.

In the hippocampus, the distribution of *Shh*⁺*nNOS*⁺ cells scattered throughout the hippocampal layers is in agreement with the distribution of nitroergic interneurons identified by NADPH diaphorase staining or immunohistochemistry (Tricoire and Vitalis 2012). Whether Shh mRNA is expressed in different types of nNOS interneurons, including VIP, calretinin, parvalbumin, or somatostatin interneurons, needs further investigation. The presence of nNOS mRNA identified in our study in the CA3 pyramidal field is in agreement with the network of nNOS-immunoreactive neurons in the rat (Chong et al. 2019) and in the mouse (Cork et al. 1998).

In the hypothalamus, we observed that the broad distribution of nNOS identified here by smFISH is very similar to that reported by immunohistochemistry (Chachlaki et al. 2017). Interestingly, our analyses of double-labeled structures highlight that Shh and nNOS mRNAs are abundantly co-expressed in hypothalamic nuclei, consistent with a potential role for NO signaling in modulating Shh activity. In DMH and VMH, it has been reported that 85% of nNOS-immunoreactive neurons are glutamatergic while less than 15% are GABAergic (Chachlaki et al. 2017). Thus, our data support that Shh is expressed in a large population of glutamatergic neurons as 38–56% of nNOS-positive neurons in these nuclei also express Shh mRNA. However, the Shh GABAergic neurons observed in the ARC, VMH, and DMH are also consistent with *Shh* expression in nNOS-positive cells, which are almost all GABAergic in the ARC (Chachlaki et al. 2017). *Shh* was not expressed in the few cholinergic neurons that populate these nuclei. Further studies, such as single-cell RNA sequencing, to access the molecular identity of hypothalamic Shh cell types are needed to identify which groups of GABAergic and glutamatergic neurons these cells belong to in these nuclei (Campbell et al. 2017) and in the LHA (Mickelsen et al. 2019; Rossi et al. 2019).

What are the physiological functions mediated by Shh ligand in hypothalamus? Recently, genetic activation of Shh signaling in mouse hypothalamic astrocytes has been shown to increase sensitivity to blood glucose levels and to display a major role in counteracting metabolic defects associated with aging and obesity (Tirou et al. 2021). The broad expression of Shh transcripts in multiple hypothalamic neuronal populations identified here, together with the distribution of both the precursor and the aminoterminal active fragments of Shh in hypothalamic tissues (Tirou et al. 2021), suggest that Shh signaling in astrocytes may be regulated locally to control glucose metabolism.

In addition to being expressed in the above-mentioned nuclei, *Shh* is also abundantly expressed in other

hypothalamic nuclei implicated in the regulation of energy homeostasis such as the lateral hypothalamic nucleus or the paraventricular nucleus (Chachlaki et al. 2017). However, the presence of *Shh* in GABAergic neurons in the suprachiasmatic nucleus (SCN) supports a role for the pathway in regulating circadian rhythm as recently proposed (Tu et al. 2023). *Shh* from these neurons may modulate *Hh* signaling pathway mRNAs that are altered in the SCN of *Clock* mutant mice (Wang et al. 2018) or the activity of the superior cervical ganglion to regulate *Ptc* transcription in the pineal gland (Borjigin et al. 1999).

Activation of *Shh* signaling through the injection of active *Shh* protein in rodent or primate models of Parkinson's disease has been shown to preserve TH immunoreactive neurons in the SN and dopaminergic axons in the striatum, improving motor function (Dass et al. 2002; Tsuboi and Shults 2002; Dass et al. 2005). The source of *Shh* that could signal for mediating these effects in the mesostriatal system has been unclear. We now provide further evidence that a source of *Shh* is possibly dopamine neurons of the SNc and of the VTA since almost all of these neurons expressed *Shh* in the adult mouse brain. Indeed, expression of *Shh* transcripts were not detected by us in our first studies in rat using specific digoxigenin-labeled riboprobes (Traiffort et al. 1998, 1999) or in mouse (unpublished observations), and was not reported by others using reporter mouse lines (Ihrle et al. 2011). *Shh* protein has not been reported, to our knowledge, in dopaminergic neurons by immunohistochemistry in adult rodent brain using *Shh* antibodies (Machold et al. 2003; Ihrle et al. 2011; Ferent et al. 2013b). Consequently, the absence of protein expression analysis in this region makes it difficult to verify consistency between transcript density and protein, an observation that may also apply to other brain regions where *Shh* protein expression analysis is absent. However, evidence for *Shh* expression by all TH neurons was observed using X-Gal staining of sections from 3-month-old mice heterozygous for a conditional, gene expression tracer allele of *Shh* (*Shh-nLacZ^{C/+}*) (Gonzalez-Reyes et al. 2012). Thus, the apparent discrepancy among these reports may reflect different sensitivity of reporters, of the mouse line constructs and of antibodies used. Of interest, genetic ablation of *Shh* in TH-expressing neurons was associated with motor deficits that might have resulted from loss of dopaminergic, cholinergic and fast spiking GABAergic neurons (Gonzalez-Reyes et al. 2012). It was postulated that GDNF was implicated in the inhibition of *Shh* expression from dopaminergic neurons. Our present data also indicate the presence of *Ptc* on dopaminergic neurons that was not identified previously, suggesting a possible cell autonomous mode of *Shh* signaling on dopaminergic neurons. However, we show that astrocytes in the VTA and the SNc expressed high levels of *Ptc* and

Smo transcripts suggesting that *Shh* signaling in astrocytes might participate in dopaminergic neurons regulation in the healthy brain and might be involved in the complex mechanisms underlying their loss during Parkinson's disease (Kery et al. 2020).

Conclusion

Although the precise distribution of *Shh* peptides needs to be further investigated in the adult rodent brain, the present results reveal that the *Shh* molecule is expressed more widely than originally thought. The widespread neuronal distribution of *Shh* mRNA in GABAergic, cholinergic, dopaminergic, nitrergic, and probably glutamatergic neurons, and its restricted expression in a population of oligodendroglial cells in almost all areas of the brain, suggest that *Shh* is an important physiological cue for astrocytes, which are the major *Shh*-responsive cells in the brain. Thus, *Shh* from neuronal sources may act locally or after transport to act on specific astrocyte populations to mediate anti-inflammatory actions or regulate energy metabolism (Garcia 2021; Tirou et al. 2021). However, as the transcription factor *Gli1* is not expressed in neurons, *Shh* could act on neuronal *Ptc* (Traiffort et al. 1999) through non-canonical signaling to regulate neuronal functions and potentially the expression of *Shh* and *Shh* regulators (Loulier et al. 2005; Allahyari et al. 2019). Future physiological studies should be undertaken to examine how *Shh* mRNA and peptides are regulated from neuronal and oligodendroglial sources in healthy and pathological states. Such studies could not only provide a better understanding of the functions of *Shh* signaling in normal and pathological states, but also identify new regulatory mechanisms that could be targets for new drugs.

Supplementary Information The online version contains supplementary material available at <https://doi.org/10.1007/s00429-023-02756-2>.

Author contributions RM, SA, and RM designed the study. RM, GP, HF, and LT completed the experiments and RM run the analyses. RM and RM wrote the manuscript. All authors reviewed the final version of the manuscript for intellectual content.

Funding M. Russo is recipient of a doctoral grant from the French Ministry of Research and the Foundation for Medical Research. This work was supported by grants from Foundation ARSEP (Aide à la Recherche sur la Sclérose En Plaques) to M. Ruat.

Data availability Contact the corresponding author to access the primary data material.

Declarations

Conflict of interest The authors have no conflicts of interest.

Ethics approval All experimental procedures were performed in accordance with the Council Directive 2010/63/EU of the European Parliament and were approved (project n°4558) by the French ethic committee.

Consent to participate Not applicable.

Consent for publication The authors give consent for publication.

Open Access This article is licensed under a Creative Commons Attribution 4.0 International License, which permits use, sharing, adaptation, distribution and reproduction in any medium or format, as long as you give appropriate credit to the original author(s) and the source, provide a link to the Creative Commons licence, and indicate if changes were made. The images or other third party material in this article are included in the article's Creative Commons licence, unless indicated otherwise in a credit line to the material. If material is not included in the article's Creative Commons licence and your intended use is not permitted by statutory regulation or exceeds the permitted use, you will need to obtain permission directly from the copyright holder. To view a copy of this licence, visit <http://creativecommons.org/licenses/by/4.0/>.

References

- Allahyari RV, Clark KL, Shepard KA, Garcia ADR (2019) Sonic hedgehog signaling is negatively regulated in reactive astrocytes after forebrain stab injury. *Sci Rep* 9:565
- Alvarez-Buylla A, Ihrie RA (2014) Sonic hedgehog signaling in the postnatal brain. *Semin Cell Dev Biol* 33:105–111
- Andreu-Cervera A, Catala M, Schneider-Maunoury S (2021) Cilia, ciliopathies and hedgehog-related forebrain developmental disorders. *Neurobiol Dis* 150:105236
- Angot E, Loulier K, Nguyen-Ba-Charvet KT, Gadeau AP, Ruat M, Traiffort E (2008) Chemoattractive activity of sonic hedgehog in the adult subventricular zone modulates the number of neural precursors reaching the olfactory bulb. *Stem Cells* 26:2311–2320
- Antonellis PJ, Engle SE, Brewer KM, Berbari NF (2021) The Hedgehog signaling pathway is expressed in the adult mouse hypothalamus and modulated by fasting. *eNeuro* 8
- Barbosa IM, Ferrante SM, Mandarim-De-Lacerda CA (2001) Role of nitric oxide synthase in the etiopathogenesis of hypertrophic pyloric stenosis in infants. *J Pediatr (Rio J)* 77:307–312
- Borjigin J, Deng J, Wang MM, Li X, Blackshaw S, Snyder SH (1999) Circadian rhythm of patched1 transcription in the pineal regulated by adrenergic stimulation and cAMP. *J Biol Chem* 274:35012–35015
- Briscoe J, Therond PP (2013) The mechanisms of Hedgehog signalling and its roles in development and disease. *Nat Rev* 14:416–429
- Campbell EJ, Barker DJ, Nasser HM, Kaganovsky K, Dayas CV, Marchant NJ (2017) Cue-induced food seeking after punishment is associated with increased Fos expression in the lateral hypothalamus and basolateral and medial amygdala. *Behav Neurosci* 131:155–167
- Chachlaki K, Malone SA, Qualls-Creekmore E, Hrabovszky E, Muzberg H, Giacobini P, Ango F, Prevot V (2017) Phenotyping of nNOS neurons in the postnatal and adult female mouse hypothalamus. *J Comp Neurol* 525:3177–3189
- Charytoniuk D, Porcel B, Rodriguez Gomez J, Faure H, Ruat M, Traiffort E (2002) Sonic Hedgehog signalling in the developing and adult brain. *J Physiol Paris* 96:9–16
- Chong PS, Poon CH, Fung ML, Guan L, Steinbusch HWM, Chan YS, Lim WL, Lim LW (2019) Distribution of neuronal nitric oxide synthase immunoreactivity in adult male Sprague-Dawley rat brain. *Acta Histochem* 121:151437
- Cork RJ, Perrone ML, Bridges D, Wandell J, Scheiner CA, Mize RR (1998) A web-accessible digital atlas of the distribution of nitric oxide synthase in the mouse brain. *Prog Brain Res* 118:37–50
- Dass B, Irvani MM, Jackson MJ, Engber TM, Galdes A, Jenner P (2002) Behavioural and immunohistochemical changes following supranigral administration of sonic hedgehog in 1-methyl-4-phenyl-1,2,3,6-tetrahydropyridine-treated common marmosets. *Neuroscience* 114:99–109
- Dass B, Irvani MM, Huang C, Barsoum J, Engber TM, Galdes A, Jenner P (2005) Sonic hedgehog delivered by an adeno-associated virus protects dopaminergic neurones against 6-OHDA toxicity in the rat. *J Neural Transm (Vienna)* 112:763–778
- Del Giovane A, Russo M, Tirou L, Faure H, Ruat M, Balestri S, Spasato C, Basoli F, Rainer A, Kassoussi A, Traiffort E, Ragnini-Wilson A (2022) Smoothed/AMP-activated protein kinase signaling in oligodendroglial cell maturation. *Front Cell Neurosci* 15:17
- Desouza LA, Sathanoori M, Kapoor R, Rajadhyaksha N, Gonzalez LE, Kottmann AH, Tole S, Vaidya VA (2011) Thyroid hormone regulates the expression of the sonic hedgehog signaling pathway in the embryonic and adult mammalian brain. *Endocrinology* 152:1989–2000
- Eitan E, Petralia RS, Wang YX, Indig FE, Mattson MP, Yao PJ (2016) Probing extracellular Sonic hedgehog in neurons. *Biol Open* 5:1086–1092
- Farmer WT, Abrahamsson T, Chierzi S, Lui C, Zaelzer C, Jones EV, Bally BP, Chen GG, Theroux JF, Peng J, Bourque CW, Charon F, Ernst C, Sjöström PJ, Murai KK (2016) Neurons diversify astrocytes in the adult brain through sonic hedgehog signaling. *Science* 351:849–854
- Ferent J, Ruat M, Traiffort E (2013a) Investigation of the proteolipid protein promoter activity during demyelination and repair. *Differentiation* 85:182–189
- Ferent J, Zimmer C, Durbec P, Ruat M, Traiffort E (2013b) Sonic Hedgehog signaling is a positive oligodendrocyte regulator during demyelination. *J Neurosci* 33:1759–1772
- Garcia ADR (2021) New tricks for an old (hedge)hog: sonic hedgehog regulation of astrocyte function. *Cells* 10:1353
- Garcia AD, Petrova R, Eng L, Joyner AL (2010) Sonic hedgehog regulates discrete populations of astrocytes in the adult mouse forebrain. *J Neurosci* 30:13597–13608
- Garcia ADR, Han YG, Triplett JW, Farmer WT, Harwell CC, Ihrie RA (2018) The elegance of sonic hedgehog: emerging novel functions for a classic morphogen. *J Neurosci* 38:9338–9345
- Gerashchenko D, Wisor JP, Burns D, Reh RK, Shiromani PJ, Sakurai T, de la Iglesia HO, Kilduff TS (2008) Identification of a population of sleep-active cerebral cortex neurons. *Proc Natl Acad Sci USA* 105:10227–10232
- Gonzalez-Reyes LE, Verbitsky M, Blesa J, Jackson-Lewis V, Paredes D, Tillack K, Phani S, Kramer ER, Przedborski S, Kottmann AH (2012) Sonic hedgehog maintains cellular and neurochemical homeostasis in the adult nigrostriatal circuit. *Neuron* 75:306–319
- Gonzalez-Reyes LE, Chiang CC, Zhang M, Johnson J, Arrillaga-Tamez M, Couturier NH, Reddy N, Starikov L, Capadona JR, Kottmann AH, Durand DM (2019) Sonic Hedgehog is expressed by hilar mossy cells and regulates cellular survival and neurogenesis in the adult hippocampus. *Sci Rep* 9:17402
- Haag D, Zipper P, Westrich V, Karra D, Pflieger K, Toedt G, Blond F, Delhomme N, Hahn M, Reifenberger J, Reifenberger G, Lichter P (2012) Nos2 inactivation promotes the development

- of medulloblastoma in *Ptch1*(+/-) mice by deregulation of Gap43-dependent granule cell precursor migration. *PLoS Genet* 8:e1002572
- Harwell CC, Parker PR, Gee SM, Okada A, McConnell SK, Kreitzer AC, Kriegstein AR (2012) Sonic hedgehog expression in corticofugal projection neurons directs cortical microcircuit formation. *Neuron* 73:1116–1126
- Hill SA, Blaaser AS, Coley AA, Xie Y, Shepard KA, Harwell CC, Gao WJ, Garcia ADR (2019) Sonic hedgehog signaling in astrocytes mediates cell-type-specific synaptic organization. *Elife* 8:e45545
- Hrabovszky E, Wittmann G, Kallo I, Fuzesi T, Fekete C, Liposits Z (2012) Distribution of type I cannabinoid receptor-expressing neurons in the septal-hypothalamic region of the mouse: colocalization with GABAergic and glutamatergic markers. *J Comp Neurol* 520:1005–1020
- Ihrig RA, Shah JK, Harwell CC, Levine JH, Guinto CD, Lezama M, Kriegstein AR, Alvarez-Buylla A (2011) Persistent sonic hedgehog signaling in adult brain determines neural stem cell positional identity. *Neuron* 71:250–262
- Karagiannis A, Gallopin T, David C, Battaglia D, Geoffroy H, Rossier J, Hillman EM, Staiger JF, Cauli B (2009) Classification of NPY-expressing neocortical interneurons. *J Neurosci* 29:3642–3659
- Kery R, Chen APF, Kirschen GW (2020) Genetic targeting of astrocytes to combat neurodegenerative disease. *Neural Regen Res* 15:199–211
- Lai K, Kaspar BK, Gage FH, Schaffer DV (2003) Sonic hedgehog regulates adult neural progenitor proliferation in vitro and in vivo. *Nat Neurosci* 6:21–27
- Laouarem Y, Traiffort E (2018) Developmental and repairing production of myelin: the role of hedgehog signaling. *Front Cell Neurosci* 12:305
- Laouarem Y, Kassoussi A, Zahaf A, Hutteau-Hamel T, Mellouk A, Bobe P, Mattern C, Schumacher M, Traiffort E (2021) Functional cooperation of the hedgehog and androgen signaling pathways during developmental and repairing myelination. *Glia* 69:1369–1392
- Lee JE, Jeon CJ (2005) Immunocytochemical localization of nitric oxide synthase-containing neurons in mouse and rabbit visual cortex and co-localization with calcium-binding proteins. *Mol Cells* 19:408–417
- Lier J, Streit WJ, Bechmann I (2021) Beyond activation: characterizing microglial functional phenotypes. *Cells* 10:2236
- Loulier K, Ruat M, Traiffort E (2005) Analysis of hedgehog interacting protein in the brain and its expression in nitric oxide synthase-positive cells. *NeuroReport* 16:1959–1962
- Loulier K, Ruat M, Traiffort E (2006) Increase of proliferating oligodendroglial progenitors in the adult mouse brain upon Sonic hedgehog delivery in the lateral ventricle. *J Neurochem* 98:530–542
- Machold R, Hayashi S, Rutlin M, Muzumdar MD, Nery S, Corbin JG, Gritti-Linde A, Dellovade T, Porter JA, Rubin LL, Dudek H, McMahon AP, Fishell G (2003) Sonic hedgehog is required for progenitor cell maintenance in telencephalic stem cell niches. *Neuron* 39:937–950
- Malave L, Zuelke DR, Uribe-Cano S, Starikov L, Rebholz H, Friedman E, Qin C, Li Q, Bezaud E, Kottmann AH (2021) Dopaminergic co-transmission with sonic hedgehog inhibits abnormal involuntary movements in models of Parkinson's disease and L-Dopa induced dyskinesia. *Commun Biol* 4:1071
- McMahon AP, Ingham PW, Tabin CJ (2003) Developmental roles and clinical significance of hedgehog signaling. *Curr Top Dev Biol* 53:1–114
- Mickelsen LE, Bolisetty M, Chimileski BR, Fujita A, Beltrami EJ, Costanzo JT, Naparstek JR, Robson P, Jackson AC (2019) Single-cell transcriptomic analysis of the lateral hypothalamic area reveals molecularly distinct populations of inhibitory and excitatory neurons. *Nat Neurosci* 22:642–656
- Oermann E, Bidmon HJ, Mayer B, Zilles K (1999) Differential maturational patterns of nitric oxide synthase-I and NADPH diaphorase in functionally distinct cortical areas of the mouse cerebral cortex. *Anat Embryol (berl)* 200:27–41
- Okuda H, Tatsumi K, Morita-Takemura S, Nakahara K, Nochioka K, Shinjo T, Terada Y, Wanaka A (2016) Hedgehog signaling modulates the release of gliotransmitters from cultured cerebellar astrocytes. *Neurochem Res* 41:278–289
- Olah S, Fule M, Komlosi G, Varga C, Baldi R, Barzo P, Tamas G (2009) Regulation of cortical microcircuits by unitary GABA-mediated volume transmission. *Nature* 461:1278–1281
- Pascual O, Traiffort E, Baker DP, Galdes A, Ruat M, Champagnat J (2005) Sonic hedgehog signalling in neurons of adult ventrolateral nucleus tractus solitarius. *Eur J Neurosci* 22:389–396
- Paxinos G, Franklin KBJ (2001) The mouse brain in stereotaxic coordinates. Academic Press, London
- Perrenoud Q, Geoffroy H, Gauthier B, Rancillac A, Alfonsi F, Kessar N, Rossier J, Vitalis T, Gallopin T (2012) Characterization of type I and type II nNOS-expressing interneurons in the barrel cortex of mouse. *Front Neural Circuits* 6:36
- Porcu G, Serone E, De Nardis V, Di Giandomenico D, Lucisano G, Scardapane M, Poma A, Ragnini-Wilson A (2015) Clobetasol and halcinonide act as smoothened agonists to promote myelin gene expression and R γ receptor activation. *PLoS ONE* 10:e0144550
- Reifenberger J, Wolter M, Weber RG, Megahed M, Ruzicka T, Lichter P, Reifenberger G (1998) Missense mutations in SMOH in sporadic basal cell carcinomas of the skin and primitive neuroectodermal tumors of the central nervous system. *Cancer Res* 58:1798–1803
- Rivell A, Petralia RS, Wang YX, Clawson E, Moehl K, Mattson MP, Yao PJ (2019) Sonic hedgehog expression in the postnatal brain. *Biol Open* 8:040592
- Robertson CP, Gibbs SM, Roelink H (2001) cGMP enhances the sonic hedgehog response in neural plate cells. *Dev Biol* 238:157–167
- Rossi MA, Basiri ML, McHenry JA, Kosyk O, Otis JM, van den Munkhof HE, Bryois J, Hubel C, Breen G, Guo W, Bulik CM, Sullivan PF, Stuber GD (2019) Obesity remodels activity and transcriptional state of a lateral hypothalamic brake on feeding. *Science* 364:1271–1274
- Ruat M, Hoch L, Faure H, Rognan D (2014) Targeting of Smoothened for therapeutic gain. *Trends Pharmacol Sci* 35:237–246
- Ruat M, Faure H, Daynac M (2015) Smoothened, stem cell maintenance and brain diseases. *Top Med Chem* 16:147–171
- Samanta J, Grund EM, Silva HM, Lafaille JJ, Fishell G, Salzer JL (2015) Inhibition of Gli1 mobilizes endogenous neural stem cells for remyelination. *Nature* 526:448–452
- Sanchez MA, Armstrong RC (2018) Postnatal Sonic hedgehog (Shh) responsive cells give rise to oligodendrocyte lineage cells during myelination and in adulthood contribute to remyelination. *Exp Neurol* 299:122–136
- Sanchez MA, Sullivan GM, Armstrong RC (2018) Genetic detection of Sonic hedgehog (Shh) expression and cellular response in the progression of acute through chronic demyelination and remyelination. *Neurobiol Dis* 115:145–156
- Swiderska-Syn M, Mir-Pedrol J, Oles A, Schleuger O, Salvador AD, Greiner SM, Seward C, Yang F, Babcock BR, Shen C, Wynn DT, Sanchez-Mejias A, Gershon TR, Martin V, McCrea HJ, Lindsey KG, Krieg C, Rodriguez-Blanco J (2022) Noncanonical activation of GLI signaling in SOX2(+) cells drives medulloblastoma relapse. *Sci Adv* 8:eabj9138

- Tirou L, Russo M, Faure H, Pellegrino G, Sharif A, Ruat M (2020) C9C5 positive mature oligodendrocytes are a source of Sonic Hedgehog in the mouse brain. *PLoS ONE* 15:e0229362
- Tirou L, Russo M, Faure H, Pellegrino G, Demongin C, Daynac M, Sharif A, Amosse J, Le Lay S, Denis R, Luquet S, Taouis M, Benomar Y, Ruat M (2021) Sonic Hedgehog receptor patched deficiency in astrocytes enhances glucose metabolism in mice. *Mol Metab* 47:101172
- Traiffort E, Charytoniuk DA, Faure H, Ruat M (1998) Regional distribution of Sonic Hedgehog, patched, and smoothened mRNA in the adult rat brain. *J Neurochem* 70:1327–1330
- Traiffort E, Charytoniuk D, Watroba L, Faure H, Sales N, Ruat M (1999) Discrete localizations of hedgehog signalling components in the developing and adult rat nervous system. *Eur J Neurosci* 11:3199–3214
- Traiffort E, Moya KL, Faure H, Hassig R, Ruat M (2001) High expression and anterograde axonal transport of aminoterminal sonic hedgehog in the adult hamster brain. *Eur J Neurosci* 14:839–850
- Traiffort E, Dubourg C, Faure H, Rognan D, Odent S, Durou MR, David V, Ruat M (2004) Functional characterization of sonic hedgehog mutations associated with holoprosencephaly. *J Biol Chem* 279:42889–42897
- Tricoire L, Vitalis T (2012) Neuronal nitric oxide synthase expressing neurons: a journey from birth to neuronal circuits. *Front Neural Circuits* 6:82
- Tsuboi K, Shults CW (2002) Intrastriatal injection of sonic hedgehog reduces behavioral impairment in a rat model of Parkinson's disease. *Exp Neurol* 173:95–104
- Tu HQ, Li S, Xu YL, Zhang YC, Li PY, Liang LY, Song GP, Jian XX, Wu M, Song ZQ, Li TT, Hu HB, Yuan JF, Shen XL, Li JN, Han QY, Wang K, Zhang T, Zhou T, Li AL, Zhang XM, Li HY (2023) Rhythmic cilia changes support SCN neuron coherence in circadian clock. *Science* 380:972–979
- Turcato FC, Wegman E, Lu T, Ferguson N, Luo Y (2022) Dopaminergic neurons are not a major Sonic hedgehog ligand source for striatal cholinergic or PV interneurons. *iScience* 25:105278
- Vercelli A, Garbossa D, Biasiol S, Repici M, Jhaveri S (2000) NOS inhibition during postnatal development leads to increased ipsilateral retinocollicular and retinogeniculate projections in rats. *Eur J Neurosci* 12:473–490
- Wallace VA (1999) Purkinje-cell-derived Sonic hedgehog regulates granule neuron precursor cell proliferation in the developing mouse cerebellum. *Curr Biol* 9:445–448
- Wang Y, Lv K, Zhao M, Liang F, Chen H, Ji G, Wang T, Zhang Y, Cao H, Li Y, Qu L (2018) Expression profiles and functional annotation analysis of mRNAs in suprachiasmatic nucleus of Clock mutant mice. *Gene* 647:107–114
- Wang H, Xu Z, Xia Z, Rallo M, Duffy A, Matisse MP (2021) Inactivation of Hedgehog signal transduction in adult astrocytes results in region-specific blood-brain barrier defects. *Proc Natl Acad Sci USA* 118:e2017779118
- Wiencken AE, Casagrande VA (2000) The distribution of NADPH diaphorase and nitric oxide synthetase (NOS) in relation to the functional compartments of areas V1 and V2 of primate visual cortex. *Cereb Cortex* 10:499–511
- Wolter M, Reifenberger J, Sommer C, Ruzicka T, Reifenberger G (1997) Mutations in the human homologue of the *Drosophila* segment polarity gene patched (PTCH) in sporadic basal cell carcinomas of the skin and primitive neuroectodermal tumors of the central nervous system. *Cancer Res* 57:2581–2585
- Yao PJ, Petralia RS, Mattson MP (2016) Sonic Hedgehog signaling and hippocampal neuroplasticity. *Trends Neurosci* 39:840–850
- Zhang Y, Beachy PA (2023) Cellular and molecular mechanisms of Hedgehog signalling. *Nat Rev* 24:668–687
- Zhang D, Wang H, Liu H, Tao T, Wang N, Shen A (2016) nNOS translocates into the nucleus and interacts with Sox2 to protect neurons against early excitotoxicity via promotion of Shh transcription. *Mol Neurobiol* 53:6444–6458

Publisher's Note Springer Nature remains neutral with regard to jurisdictional claims in published maps and institutional affiliations.